6-30-2016

Investigation of Succinated Protein Turnover by Autophagy

Lydia Proctor
University of South Carolina

Investigation of Succinated Protein Turnover by Autophagy

by

Lydia Proctor

Bachelor of Science
University of Michigan, 2014

Submitted in Partial Fulfillment of the Requirements

For the Degree of Master of Science in

Biomedical Science

School of Medicine

University of South Carolina

2016

Accepted by:

Norma Frizzell, Director of Thesis

Pavel Ortinski, Reader

Daping Fan, Reader

Lacy Ford, Senior Vice Provost and Dean of Graduate Studies

Acknowledgements

I would like to thank my mentor, Dr. Norma Frizzell, for her continued guidance and understanding. Her dedication to my individual success and this project was invaluable at each step in my graduate education at the University of South Carolina. I also want to thank my committee members Dr. Daping Fan and Dr. Pavel Ortinski for their assistance with the completion of my thesis.

I am thankful for my lab members' daily support and encouragement: to Dr. Gerardo Piroli for his expert advice and patience in teaching; to Allison Manuel for her time devoted to teaching me new techniques and assistance in data collection and analysis; to Scott Lanci for his willingness to help in lab and in navigating the MS process; and to Anna Clapper for her involvement in training me and availability to aid with experiments.

Finally I would like to thank my friends and family who made this all possible: to my fiancé Jake for his encouragement and continued emotional support; to my parents for their devotion to my academic success from a young age; to my siblings Dan and Carolyn for their continued support; to my roommates Kristy and Mary; and to my church family at Midlands. I am blessed to have so many encouraging and positive people in my life that highlight my God-given abilities.

Abstract

Background. Diabetes is a widespread public health concern that alters the metabolism of adipocytes through high glucose stress and hormonal dysregulation. Under diabetic conditions there are excess nutrients available and subsequently an accumulation of tricarboxylic acid cycle intermediates such as fumarate. Fumarate can irreversibly react with protein cysteine residues to form S-2-succinocysteine (2SC, protein succination). Succinated proteins can be turned over by autophagy, a mechanism of removing damaged proteins and organelles that have accumulated due to metabolic stress.

Purpose. The basal flux through autophagy in adipocytes matured in non-diabetic and diabetic conditions was examined to determine the turnover of succinated proteins. Additionally, fumarase content was reduced using a shRNA lentiviral knockdown to elevate fumarate levels. This model of enhanced succination was used to assess autophagic flux and succinated protein turnover in the total homogenate and enriched fractions of the cytosol, mitochondria, and nucleus.

Methods. 3T3-L1 fibroblasts were differentiated to adipocytes then matured in normal or high glucose conditions. Using total cell lysates, I assessed 2SC and autophagic flux via western blotting. Additionally, I knocked down fumarase (*Fh* k/d) in 3T3-L1 fibroblasts, differentiated them to adipocytes, and evaluated

differences in 2SC and autophagic flux both in the total homogenate and in individual cellular fractions.

Conclusions. I conclude that succinated proteins are turned over by autophagy, but that flux through autophagy is reduced under high glucose conditions. Similarly, when succination is enhanced in adipocytes by *Fh* k/d, autophagic flux is reduced. Despite this, succinated protein turnover by autophagy occurs at a faster rate in the mitochondrial enriched fraction verses other fractions of *Fh* k/d adipocytes. These results provide insight on how metabolic dysregulation and protein modification may contribute to reduced autophagy under diabetic conditions and confirm the utility of 2SC as a marker for high glucose stress.

Table of Contents

List of Figures

Chapter I

INTRODUCTION

1.1. Public Health Dilemma

Metabolic syndrome is defined as the presence of at least three of the following: large waistline (≥ 40 inches for men or 35 inches for women), high triglycerides (≥ 150 mg/dL), low HDL cholesterol (≤ 40 mg/dL for men or 50 mg/dL for women), high blood pressure (systolic ≥ 130 mm Hg or diastolic ≥ 85 mm Hg), and high fasting blood glucose (≥ 100 mg/dL). The presence of these risk factors indicates increased risk for the development of heart disease, diabetes, and stroke. Type 2 diabetes mellitus (T2DM) and obesity are predominantly lifestyle-induced metabolic dysfunctions, derived from the combined effects of excessive caloric intake and increased sedentary behavior. Current Centers for Disease Control statistics show that 9.3% of the US population suffer from diabetes, 28.3% of adults are obese, and an additional 35.5% of adults are overweight (CDC). The prevention and treatment of these conditions is a national health crisis that requires immediate attention. Since T2DM and obesity are systemic, their effects on metabolic dysfunction are observed in many organs including the adipose tissue, liver, and muscle. As the disease progresses, other organs including the kidneys, heart, and eyes are also affected by diabetic complications. Therefore, a detailed mechanistic understanding of the cellular processes contributing to dysregulated metabolism

in these organs is required. In particular, the importance of maintaining metabolically healthy adipose tissue has received increased attention considering its roles in energy storage and hormone production.

1.2. Adipose Tissue

Adipose tissue is a specialized tissue in which the body stores extra energy as triglycerides or releases free fatty acids in the presence of an energy deficit. This unique role allows cellular lipid droplet storage without lipotoxicity (Konige et al. 2014). This process is highly regulated by hormones that respond to the changing metabolic needs of the body. In the absence of immediately available nutrients, such as during the fasted state, glucagon and epinephrine will be released leading to lipolysis and the mobilization of energy-rich fatty acids. In contrast, during energy surplus, insulin antagonizes fuel mobilization and promotes the synthesis and storage of triglycerides in the adipocytes. The significant endocrine function of the adipocyte also contributes to the regulation of energy balance. Adipocyte hormones (adipokines) are secreted from the adipocyte and have roles in the regulation of satiety (leptin) and mediating insulin sensitive effects on muscle and liver (adiponectin) (Diez and Iglesias, 2003). Therefore, the combined actions of the adipocyte in the storage of surplus energy and systemic fuel utilization demonstrate its importance in systemic energy homeostasis.

Adipocyte metabolism is altered in diseases states such as obesity and T2DM that compromise adipose tissue homeostasis. Obesity is a chronic state of nutrient excess that results in adipocyte enlargement. This adipocyte hypertrophy

eventually leads to cell death as well as lipid accumulation in non-adipose tissues such as muscle and liver (Giordano et al. 2013, Petersen et al. 2005, Sinha et al. 2002). Dying adipocytes release fatty acids into the circulation that can be taken up by the liver, contributing to hepatic steatosis (Alkhouri et al. 2010). Treatment with PPARγ agonists, the thiazolidinediones (TZDs), induces adipogenesis and improves insulin action in both muscle and liver by promoting the redistribution of fat out of these tissues and into peripheral adipocytes. The induction of PPARγ in adipocytes alone is sufficient to improve whole-body insulin sensitivity (Lehmann et al. 1995, Mayerson et al. 2002, Sugii et al. 2009).

The development of T2DM and reduced insulin sensitivity has been linked to metabolic stresses induced by nutrient excess, when the fuel supply exceeds the demands of the adipocyte (Keller and Attie, 2010). This results in increased intra-adipocyte stress in organelles such as the endoplasmic reticulum (ER) and the mitochondria. (Choo et al. 2006, Frizzell et al. 2012, Gregor and Hotamisligil 2007, Lin et al. 2005). Mitochondrial stress is increased under high glucose conditions as adipogenesis is occurring (Frizzell et al. 2012, Nagai et al. 2007). These metabolic stressors produce oxidative stress that induces cellular dysfunction.

Mitochondrial oxidative stress is believed to have an important role in mediating adipocyte dysfunction (Frizzell et al. 2012, Lin et al. 2005). These conditions of oxidative stress can lead to the post-translational modification of proteins, impairing their normal function. The carbonylation of adipocyte proteins by hydroxynonenal (HNE), a product of lipid oxidation, has been demonstrated in

adipocytes under diabetic conditions (Grimsrud et al. 2007, Tang et al. 2012). Recently, our laboratory has documented a new irreversible protein modification that is increased in adipocytes in high glucose conditions (see Section 1.3 below). Overall, the investigation of the biochemical changes occurring in the adipocyte under developing diabetic conditions is necessary to understand the mechanistic changes that contribute to adipocyte dysfunction. A better understanding of these pathways will allow us to design better therapeutic approaches for the management of diabetes and its complications.

1.3. Protein Succination

Protein succination is a chemical modification produced following the reaction of fumarate with the sulfhydryl group of cysteine to produce a stable adduct; S-2-succinocysteine (2SC) (Alderson et al. 2006; Figure 1.1). Our laboratory has demonstrated that cellular stress induced by nutrient excess leads to an accumulation of succinated proteins. The excess glucose availability (glucotoxicity) in adipocytes induces mitochondrial stress and leads to the accumulation of ATP (Figure 1.2). This energy accumulation will feedback and inhibit oxidative phosphorylation through mitochondrial respiratory control. Since the membrane potential is elevated, the electron transport chain is inhibited so that NADH concentration is increased. This increase in NADH/NAD^+ ratio inhibits the NAD^+ dependent enzymes of the tricarboxylic acid cycle causing accumulation of metabolic intermediates such as fumarate and malate. Fumarate reacts with available cysteines to form succinated proteins. Hence, increases in

the NADH/NAD^+ ratio appear to be a critical component contributing to elevated 2SC levels. (Frizzell et al. 2012)

Protein succination is increased on ~40 proteins in adipocytes *in vitro* and *in vivo* has been demonstrated to decrease the functionality of some of these proteins (Frizzell et al. 2009). Under diabetic conditions adiponectin is succinated and subsequently has impaired ability to oligomerize, preventing its secretion (Frizzell et al. 2009). This is significant given that high molecular weight forms of adiponectin are decreased in the plasma of T2DM patients and animal models (Pajvani et al. 2004). Additionally, an important mitochondrial enzyme, glyceraldehyde 3-phosphate dehydrogenase (GAPDH), is irreversibly succinated under diabetic conditions (Blatnik et al. 2008). Succination has also been shown to target metabolic proteins in cancerous conditions such as aconitase, resulting in enzymatic inhibition (Ternette et al. 2013). While we have identified many succinated proteins and examined how succination may affect protein structure or function, we have yet to examine how succinated proteins can be turned over within the adipocyte.

Succination appears to be unique to white adipose tissue. Using tissue samples from *db/db* and *ob/ob* diabetic mice we observed that succination increased in white adipose tissue but not in other tissues. Additionally, we did not observe an increase in succination in the presence of diet induced obesity and insulin resistance where mice were not diabetic yet. We concluded that succination is only markedly elevated after the onset of T2DM, not just a result of obesity and insulin resistance. Hence, 2SC may be a marker of the progression

to diabetes. We have confirmed that the limited oxidative demands of white adipose tissue make it uniquely susceptible to the accumulation of succinated proteins. (Frizzell et al. 2012, Thomas et al. 2012)

1.4. Mechanisms of Protein Turnover

Damaged proteins are removed from the cell via one of two catabolic pathways: the ubiquitin proteasome system (UPS) or the lysosomal degradation system known as autophagy. Protein degradation is highly regulated and occurs in response to cellular stress, such as nutrient deprivation, to provide the cell with amino acids, such as alanine, that can be used for gluconeogenesis. In a healthy cell these processes maintain levels of damaged and dysfunctional proteins below a specific threshold.

The UPS is a process of degrading damaged proteins (Figure 1.3). Ubiquitin ligases E1, E2, and E3 will activate, conjugate, and then transfer ubiquitin to the unfolded or misfolded proteins. Once proteins are polyubiquitinated, i.e. have received multiple ubiquitin tags, they are targeted to the 26S proteasome. Ubiquitinated proteins are then degraded in an ATP-dependent manner by the proteasome. The resulting amino acids are then reutilized by the cell for energy or the synthesis of new proteins.

Autophagy is the process by which damaged proteins and organelles are degraded in the lysosome (Figure 1.4). Similar to the UPS, protein flux through autophagy occurs to ameliorate cellular stress induced by an accumulation of cellular debris. Autophagy induction usually occurs through the signaling cascade involving serine/threonine-protein kinase ULK1. Autophagy begins when the

autophagosome membrane encases the proteins and organelles to be degraded. Numerous autophagy related genes (Atg) are involved in the stages of membrane elongation and maturation. A critical component of autophagosome formation—and hence a commonly used marker of autophagy—is microtubule-associated protein light chain 3 (LC3) (Geisler et al. 2010). LC3 in the cytosol is present as LC3-I which is activated through lipidation with the assistance of Atg7, a 78 kDa protein containing 20 cysteine residues, to form LC3-II (Tanida et al. 2008, Glick et al. 2010, Weidberg et al. 2011). Active LC3-II formation is a necessary component of autophagosome membrane formation. Once the autophagosome has enclosed the proteins and organelles to be degraded, it fuses with the acidic lysosome and dispels its contents within the autophagolysosome (Klionsky et al. 2014, Qiao et al. 2015). Ultimately, cellular metabolites recovered from lysosomal degradation will be reutilized in the cell for energy or in protein synthesis. The process of autophagy is important for maintaining healthy organelle flux. If a cell is unable to properly regulate protein turnover and degradation under metabolically stressful conditions, it will undergo apoptosis (Jin, 2006, Mazure and Pouyssegur, 2010).

1.5. Experimental Aims

The purpose of this investigation is two-fold: (1) to examine the efficiency of autophagy in high glucose conditions and to determine if the autophagy regulator Atg7 is succinated; and (2) to determine the flux through autophagy of succinated proteins in several enriched organelle fractions in adipocytes. We hypothesized that succinated protein turnover by autophagy might be reduced in

diabetic conditions and that mitochondrial enriched fractions might have more succinated protein degradation through autophagy than other cellular fractions.

In order to mechanistically examine how succinated proteins are turned over in the adipocyte we will use the 3T3-L1 fibroblast model. They are a pre-adipogenic fibroblast cell line (Green and Kehinde, 1975) that can be differentiated and matured to adipocytes in the presence of insulin, dexamethasone, and 3-isobutylmethylxanthine. I will maintain matured adipocytes in 5 mM glucose to represent normoglycemic conditions or 30 mM glucose to represent poorly controlled diabetes. In order to enhance fumarate levels and succination in the 3T3-L1 adipocytes I have also employed a lentiviral strategy to knockdown fumarase using a shRNA (Chapter 2).

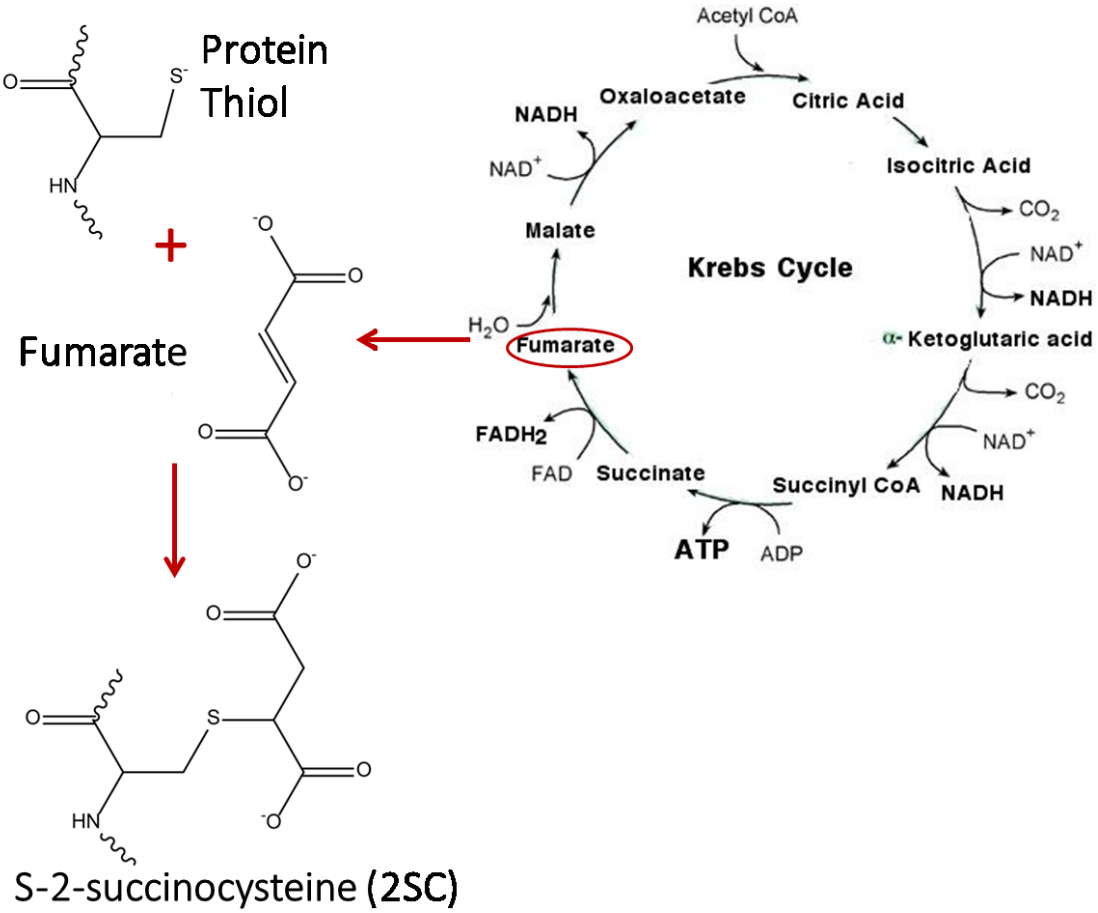

Figure 1.1. Mechanism of Protein Succination. Protein succination occurs by the reaction of the tricarboxylic acid cycle metabolic intermediate fumarate with the cysteine residue of a protein. This irreversible bond formation produces S-2-succinocysteine (2SC).

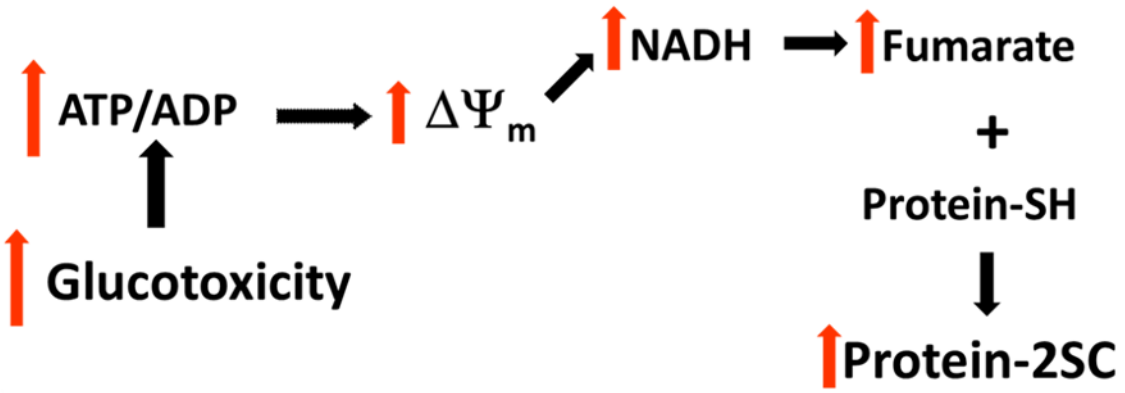

Figure 1.2. Mitochondrial Stress Leads to Protein Succination. Glucotoxicity will induce cellular stress that results in elevated protein succination. Nutrient excess (glucotoxicity) will increase the ATP/ADP ratio resulting in an elevated mitochondrial membrane potential ($\Delta\Psi_m$), increased NADH levels, and subsequently the accumulation of the tricarboxylic acid cycle intermediate fumarate. Fumarate will then react with protein thiol groups to form a succinated protein (Protein-2SC).

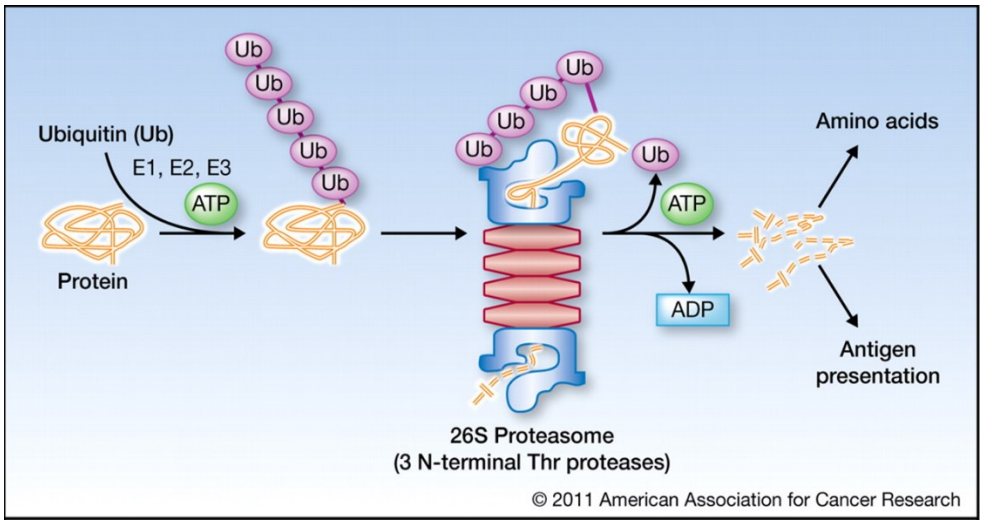

Figure 1.3. Degradation of Proteins in the Proteasome. Proteasomal protein degradation occurs when proteins become polyubiquitinated, targeting them to the 26S proteasome to be degraded into metabolites.

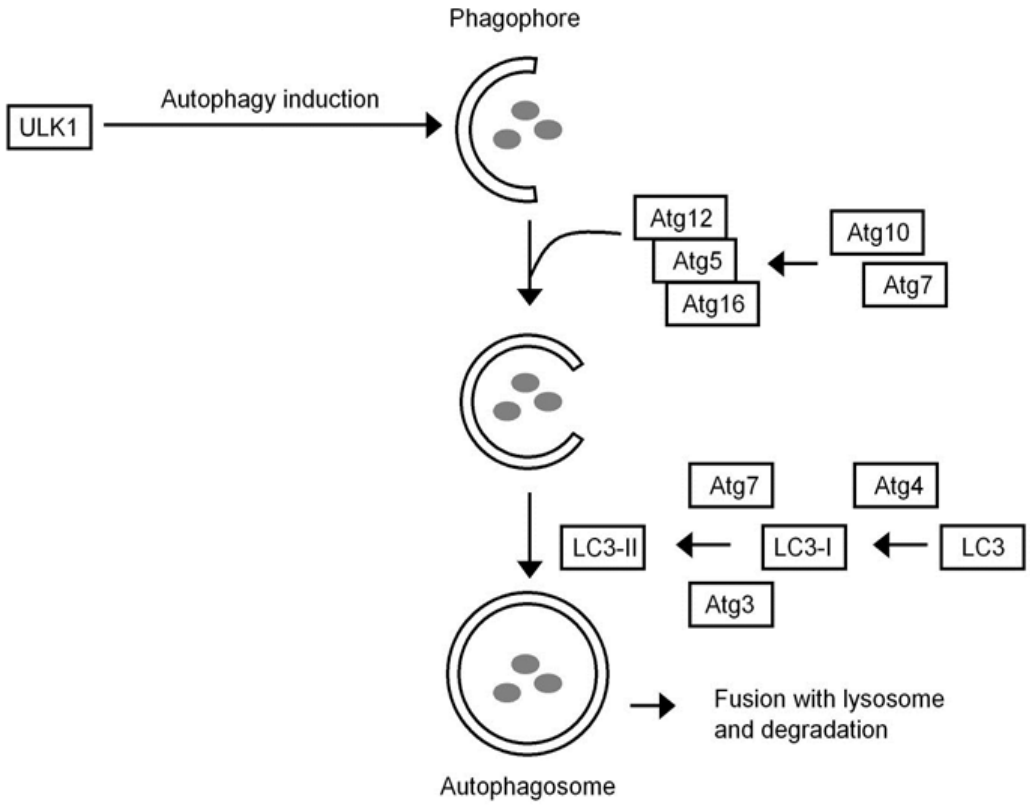

Figure 1.4. Degradation of Proteins by Autophagy. Autophagy is the lysosomal degradation of proteins and organelles. The conversion of the initial phagophore to the autophagosome occurs with the assistance of multiple autophagy related genes (Atgs) and active microtubule-associated protein light chain 3 (LC3 in the form of LC3-II) to enclose the autophagosome. The autophagosome will then fuse with the acidic lysosome where its contents will be degraded and recycled by the cell.

Chapter II

AUTOPHAGIC FLUX IN ADIPOCYTES DURING DIABETES

2.1. Introduction

Succination is an irreversible protein modification from the reaction of fumarate with cysteine to produce 2SC (Figure 1.1). When 3T3-L1 adipocytes are matured in high glucose (30 mM, diabetic conditions) for 8 days, they will accumulate succinated proteins to a greater extent than adipocytes matured in normal glucose (5 mM, non-diabetic conditions), as detected using a specific anti-2SC antibody (Nagai 2007; Frizzell 2009, 2012). However, if the adipocytes are removed from a high glucose environment for several days, succinated proteins are turned over and do not accumulate further (Frizzell et al. 2012; Figure 2.1, lanes 4-6 versus lanes 7-9). This suggests that when adipocytes are switched back to 5 mM glucose for a few days they can be rescued from the high glucose insult.

Previous research in our laboratory has further investigated the pathways mediating succinated protein turnover by inhibiting the proteasome with MG132 (carbobenzoxyl-L-leucyl-L-leucyl-L-leucinal) or inhibiting autophagy with chloroquine (CQ, drug increases lysosomal pH). These treatments were added to the growth medium of adipocytes during the last 4 days of maturation when cells were switched from high to normal glucose conditions. The turnover of succinated proteins in normal glucose was unaffected by MG132 treatment,

suggesting that the proteasome did not play a major role in succinated protein turnover (unpublished data). In contrast, when adipocytes transitioning from high glucose to normal glucose were simultaneously treated with CQ the succinated proteins appeared to accumulate (unpublished data, Figure 2.1, lanes 7-9 versus lanes 10-12). These results suggest succinated protein turnover occurs through autophagy in the adipocyte.

A parallel investigation of specific succinated proteins in adipocytes matured in high glucose has revealed that Cathepsin B, an important lysosomal protease, can be modified by 2SC. Cathepsin B is succinated on Cys108 of the occluding loop that facilitates its peptidylpepdidase activity (Illy et al. 1997, Merkley et al. 2014). We hypothesized that succination of Cys108 might contribute to reduced Cathepsin B activity and we have since demonstrated that Cathepsin B activity is reduced in high glucose conditions. In addition, this reduction can be partially recovered when adipocytes are switched to a normal glucose environment (unpublished data). Therefore, it is possible that a reduction in lysosomal protease activity as a result of Cathepsin B succination contributes to the accumulation of succination in 30 mM glucose conditions, and why succinated protein turnover is enhanced when cells are switched back to 5 mM glucose conditions.

While we understand that succinated proteins can be turned over when switched from high glucose back to normal glucose and that this occurs by autophagy over several days, we have not yet investigated the basal rates of autophagic flux in 3T3-L1 adipocytes in normal versus high glucose. This is

important as we have demonstrated that the activity of at least one lysosomal protease is decreased in high glucose. In addition, I would like to investigate another important regulator of autophagic flux, the autophagy protein ubiquitin-like modifier-activating enzyme Atg7. Atg7 is essential for the lipidation, i.e. activation, of LC3, a protein that functions in autophagosome membrane formation (Figure 1.4). Atg7 is of interest because the active site contains a cysteine residue (Cys567), therefore succination of this site on Atg7 may reduce enzymatic efficiency and impair the autophagic process.

Subsequently, I investigated (1) the profile of succinated proteins after 24 hours of 25 μM CQ administration, (2) the rate of flux through autophagy in 5 mM and 30 mM glucose conditions, and (3) Atg7 levels and its succination. I hypothesized that the rate of autophagic flux may be lower in adipocytes cultured in 30 mM glucose versus 5 mM glucose, and that Atg7 may be more succinated in cells matured in high glucose conditions.

2.2. Results

In line with our previous observations (Frizzell et al. 2012), protein succination in 3T3-L1 adipocytes is increased in high (30 mM) versus normal (5 mM) glucose conditions (Figure 2.2, lanes 1-3 versus lanes 4-6). I observed consistent levels of succination with and without CQ treatment in both 5 mM and 30 mM adipocytes (Figure 2.2, 2SC panel lanes 4-6 versus lanes 7-9 and lanes 1-3 versus 10-12). The lack of marked 2SC accumulation following 24 hours of CQ treatment is not surprising since our unpublished observations demonstrate that succinated proteins are turned over slowly, accumulating in the cell after 4

days of CQ treatment (Figure 2.1). While CQ did not markedly alter the accumulation of succinated proteins, an investigation of autophagic flux at this time point is necessary to assess the basal rate of autophagy. LC3-II levels are normally below the threshold for detection in 5 mM or 30 mM glucose conditions. However, when the cells are treated with 25 μM CQ for 24 hours to inhibit autophagy, LC3-II accumulates and autophagic flux can be determined by subtracting LC3-II levels in the presence of CQ from LC3-II levels in the absence of CQ. I observed that LC3-II accumulates in 30 mM glucose conditions and to a greater extent in 5 mM glucose conditions (Figure 2.3, LC3 panel). Therefore, these data demonstrate that basal flux through autophagy is decreased in adipocytes matured in 30 mM glucose versus 5 mM glucose (Figure 2.3, graph).

The autophagy regulating protein Atg7 is essential for the conversion of LC3 to its active form LC3-II. An initial examination of total protein levels of Atg7 suggests that Atg7 levels are reduced in adipocytes matured in 30 mM glucose versus 5 mM glucose (Figure 2.4), potentially related to the decreased lipidation of LC3 and reduced autophagic flux in 30 mM glucose conditions. In addition to this decrease, we also determined if modification of Atg7 by 2SC was occurring, potentially impairing its enzymatic activity. Enrichment of Atg7 from adipocyte whole cell lysates matured in 5 mM or 30 mM glucose by immunoprecipitation was performed. The enrichment of Atg7 was successful, as confirmed by immunoblotting with Atg7 (Figure 2.5, Atg7 panel), however, immunoblotting was unable to reliably determine if this protein is succinated as variable results were obtained, a representative image is shown (Figure 2.5, 2SC panel).

2.3. Discussion

Succinated proteins are elevated in adipocytes matured in high glucose conditions (Frizzell et al. 2012). Our results demonstrated that basal autophagic flux is reduced in cells cultured in 30 mM glucose versus those in 5 mM glucose (Figure 2.3). This inhibition of flux did not result in further accumulation of succinated proteins (Figure 2.2). We have previously illustrated that succinated protein turnover occurs slowly over several (~4) days in the presence of CQ (Figure 2.1). Therefore, these data combined with the reduced flux observation confirm that the turnover of succinated proteins is reduced in adipocytes under diabetic conditions. One possible explanation for this reduction is the succination of Cathepsin B. As described, Cathepsin B is succinated on an important cysteine residue in high glucose conditions and its enzymatic activity is reduced (Illy et al. 1997, Merkley et al. 2014, and unpublished data). It is possible that succination of additional metabolic enzymes occurs as well and contributes to a reduction in autophagic flux under high glucose stress.

Considering that LC3-II levels were lower in adipocytes matured in high glucose, we examined Atg7, the cysteine rich enzyme mediating LC3-II lipidation. Our initial immunoblotting of total levels of Atg7 provides evidence that this critical protein involved in autophagy may have reduced expression in high glucose conditions (Figure 2.3). I proposed that succination of this protein may occur on Cys567 in the active site, potentially reducing its enzymatic efficiency. In this study we were not able to conclusively determine if this protein could be succinated; this will be an area of continuing investigation in the laboratory. While

these data may have provided additional information on the source of reduced LC3-II, the study still suggests that Atg7 levels are lower in high glucose.

The accumulation of succinated proteins in high glucose conditions is representative of the metabolic stress induced by a diabetic state. Collective insults to the adipocyte during diabetes such as impaired autophagic flux (as described above), succinated protein accumulation, and oxidative stress all contribute to metabolic dysfunction. Additional evidence suggests that under diabetic conditions autophagic flux is reduced (Soussi et al. 2015). This recent study described a measurable decrease in autophagic flux of *ob/ob* (obese) mouse tissue verses *ob/+* controls. They also relate reduced autophagic flux in 3T3-L1 adipocytes to decreased mRNA expression of death associated protein kinase 2 (DAPK2), a protein proposed to modulate autophagic flux but needing further investigation. Additionally, they propose autophagic flux in human diabetic adipose tissue is reduced, providing evidence that dysregulation of flux through autophagy under a high glucose insult should be clinically investigated. A lack of sufficient protein turnover as well as impairment of succinated protein turnover may further interfere with the process of adipose tissue expansion, a normal result of nutrient excess. These forms of amplified cellular stress in high glucose foster an unhealthy environment for adipocyte expansion and subsequently may lead to cellular death. Therefore, succination is a characteristic marker of this metabolic dysregulation.

Since the turnover of damaged proteins is important for the health of the adipocyte, accumulation of succinated or oxidatively modified proteins in high

glucose conditions appears to contribute to adipocyte dysfunction. The metabolic stress induced by damaged protein accumulation is a potential source of adipose tissue inflammation. Inflammation in the adipose tissue has been linked to hypoxia (Halberg et al. 2009, Sun et al. 2013). Hypoxia has been noted as an early initiator of adipose tissue dysfunction since it is indicative of adipose tissue expansion that outpaces the growth of vasculature (Halberg et al. 2009). Additionally, hypoxia inducible factor 1 alpha (HIF-1α), a common marker of hypoxia, is decreased after weight loss (Cancello et al. 2005). In addition to high glucose stress, other factors may contribute to obesity-induced inflammation and reduced autophagic flux such as glycogen accumulation (Ceperuelo-Mallafré et al. 2016; Singh and Singh, 2015).

Overall my results suggest that autophagic flux is decreased in adipocytes under high glucose stress. This decrease may be a result of increased succination of components of the autophagic machinery and may in part explain the inability of the adipocyte to adapt to metabolic stress during diabetes.

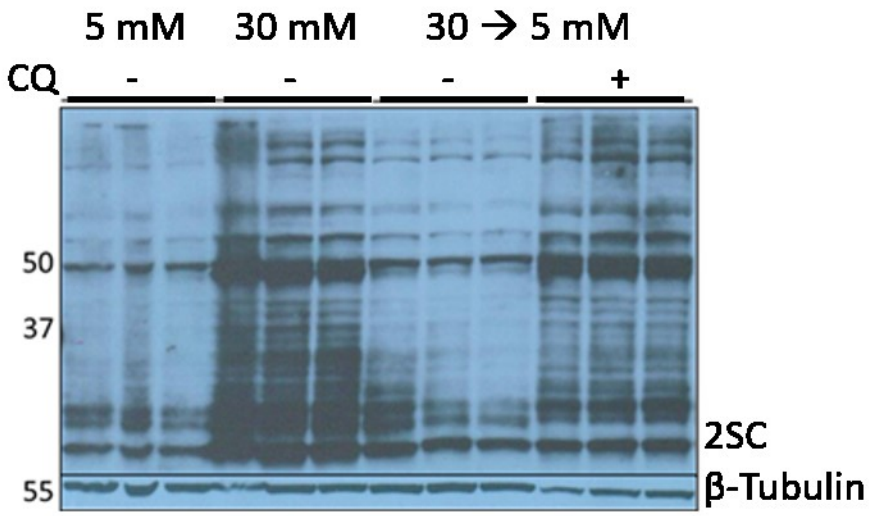

Figure 2.1. Mechanism of Succinated Protein Turnover. Succinated protein turnover occurs by autophagy. Adipocytes were matured in 5 mM or 30 mM glucose for 8 days. A subset of adipocytes were matured in 30 mM glucose for 4 days and then switched to 5 mM glucose for the remaining 4 days of maturation (30→5) and treated with or without 25 μM chloroquine. Protein 40 μg was separated by 1-D PAGE and detection of protein succination was performed using a polyclonal anti-2SC antibody (**2SC panel**). MW markers are shown in kDa and β-Tubulin is shown to demonstrate equal protein loading.

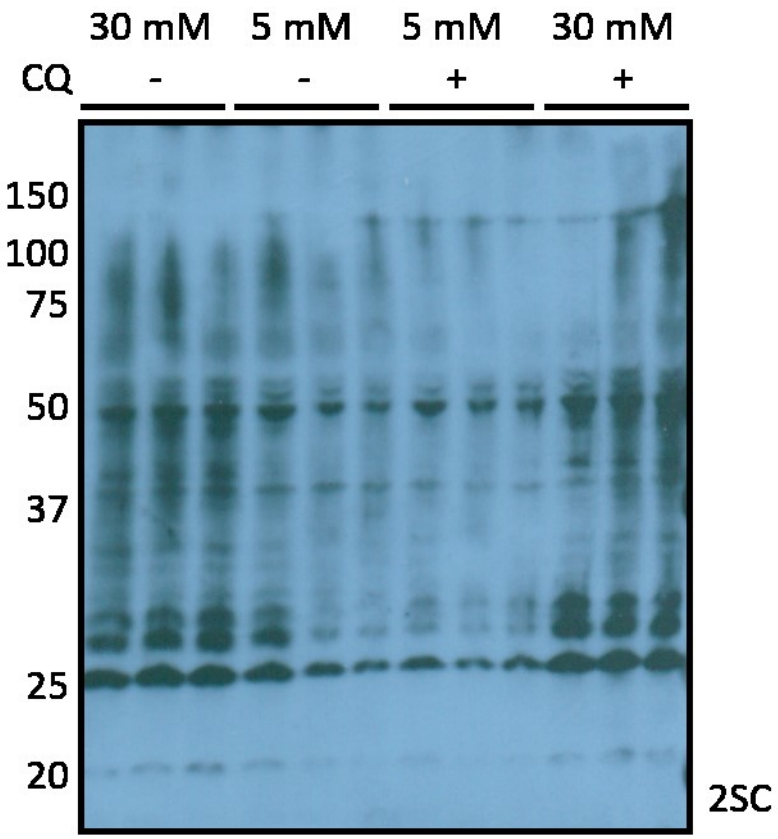

Figure 2.2. Succinated Protein Turnover by Autophagy. Adipocytes matured in 5 mM or 30 mM glucose with and without 25 μM CQ for 24 hours were assessed for succination (**2SC panel**). Total cell lysates, 30 μg protein per lane, were separated by 1-D SDS PAGE (n=3 per group). Molecular weight markers (kDa) are indicated on left.

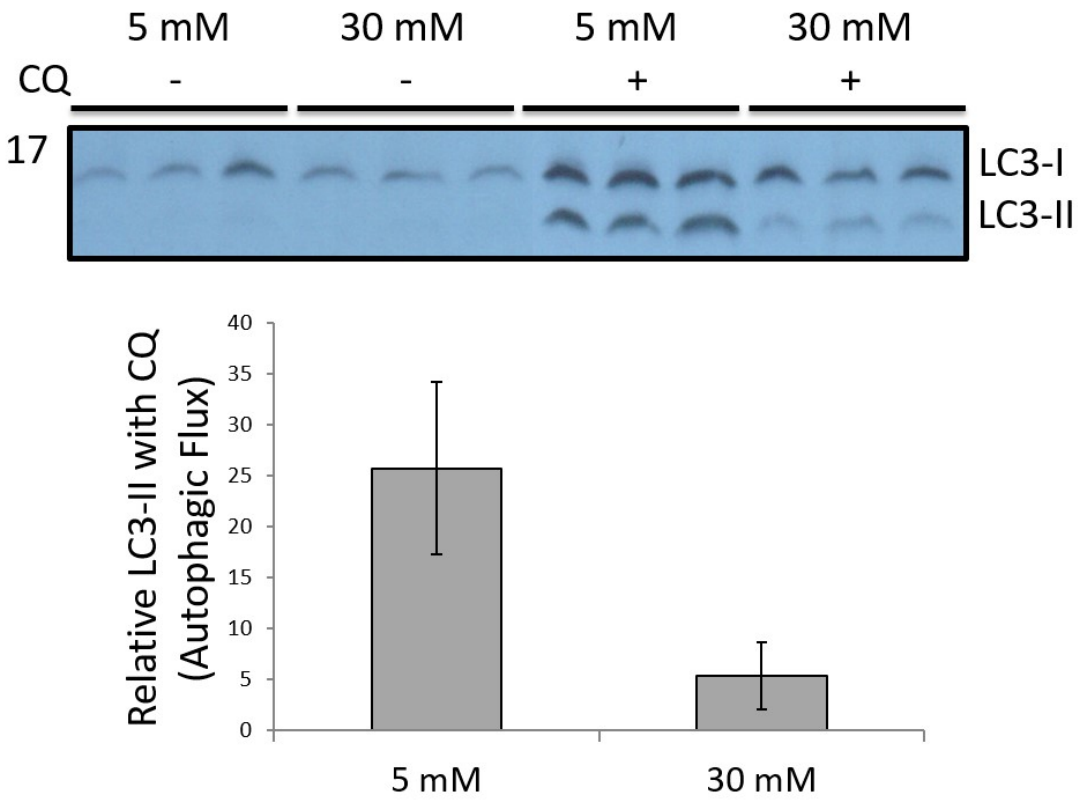

Figure 2.3. Flux through Autophagy in 3T3-L1 Adipocytes. Flux through autophagy in adipocytes grown in 5 mM or 30 mM glucose as measured by LC3-II accumulation in the presence of CQ. LC3-II levels accumulate in the presence of CQ to a greater extent in 5 mM than 30 mM glucose conditions (**LC3 panel**). The rate of flux through autophagy is reduced in 30 mM glucose conditions compared to 5 mM glucose, as determined by the densitometric subtraction of LC3-II (-CQ) from LC3-II (+CQ) (**Graph**). Representative immunoblot using 10 µg of total cell lysate protein per lane (n=3 per group). Molecular weight markers (kDa) are indicated on left.

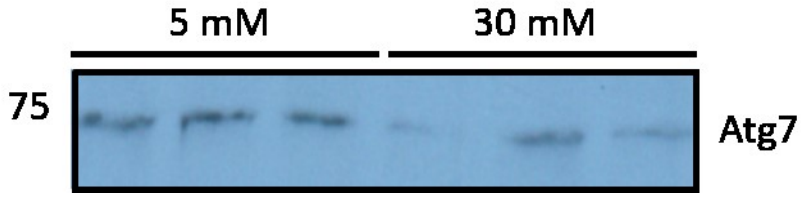

Figure 2.4. Atg7 Protein Levels. Total levels of Atg7 in adipocytes matured in 5 mM or 30 mM glucose. The levels of Atg7 are decreased in 30 mM glucose compared to 5 mM (**Atg7 panel**). Total cell lysates, 30 µg protein per lane, were separated by 1-D SDS PAGE (n=3 per group). Molecular weight marker of 75 kDa indicated on left.

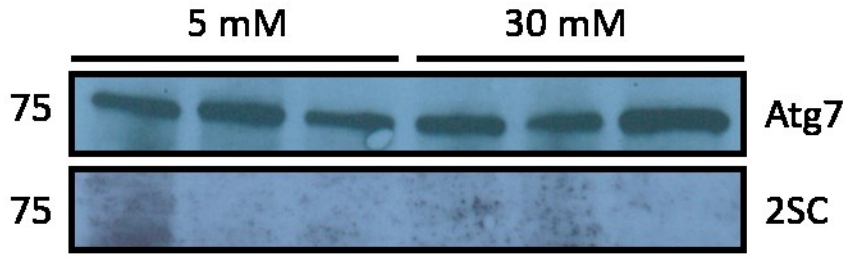

Figure 2.5. Immunoprecipitation of Atg7. Immunoprecipitation of Atg7 (anti-Atg7, Cell Signaling) from adipocytes matured in 5 mM or 30 mM glucose. Immunoprecipitation was successful in enriching relatively equal amounts of Atg7 protein from all samples (**Atg7 panel**). The blot was stripped and re-probed with anti-2SC. No detection of succination in these Atg7 precipitates (**2SC panel**). Immunoprecipitated protein samples were separated by 1-D SDS PAGE (n=3 per group). Molecular weight marker of 75 kDa indicated on left.

Chapter III

AUTOPHAGIC FLUX IN ADIPOCYTES FOLLOWING FUMARASE KNOCKDOWN

3.1. Introduction

Fumarase (FH) deficiency predisposes an individual for hereditary leiomyomatosis and renal cell cancers (HLRCC) (Pollard et al. 2005). Bi-allelic FH mutation, i.e. loss of the second copy of the FH gene, increases fumarate levels locally and is associated specifically with aggressive renal cell carcinomas (Pollard et al. 2005). Protein succination occurs when fumarate reacts with cysteine residues and results in the formation of 2SC (Alderson et al. 2006). This modification can be detected using immunohistochemistry with the anti-2SC antibody (Nagai et al. 2007). Since elevated levels of fumarate will increase protein succination, the detection of 2SC is a useful biomarker in the assessment of these FH deficient cancers (Bardella et al. 2011, Castro-Vega et al. 2014, Ternette et al. 2013, Zheng et al. 2015). Furthering our understanding of the specific metabolite and consequent protein changes induced by this fumarate accumulation may give rise to novel clinical interventions that target FH-deficient renal cell carcinomas.

Our laboratory has previously investigated a model of maximal succination using murine embryonic fibroblasts (MEFs) derived from mice with *Fh* gene knocked out (Ashrafian et al. 2010). Analysis of the cell lysate fractions

demonstrated an accumulation of succinated proteins in the total cell homogenate, but by comparison mitochondrial enriched fractions appeared to have less succination (unpublished data, Figure 3.1, lanes 1-3 versus lanes 7-9). Considering fumarate is produced and accumulates in the mitochondria, this observation was surprising. Further investigation of these *Fh*-deficient MEFs with the autophagy inhibitor chloroquine (CQ) revealed that the mitochondria did contain succinated proteins but these were rapidly turned over by autophagy (Figure 3.1, lanes 7-9 versus lanes 10-12). These data are of interest but since these are immortalized cancer cells, they may have altered autophagic flux. Since our previous observations on autophagy in adipocytes in high glucose were in 3T3-L1 cells (Chapter 2), we also wanted to prepare 3T3-L1 adipocytes with fumarase shRNA knockdown (*Fh* k/d) to better understand the role of autophagy in succinated protein turnover within enriched cellular fractions. I will utilize *Fh* k/d adipocytes to assess if the metabolic alterations present in immortalized cells are synonymous with those present in adipocytes.

To generate an adipocyte model of enhanced succination, 3T3-L1 fibroblasts were transduced with a lentiviral vector containing either fumarase shRNA or a scrambled control vector. The cells that successfully incorporated the vector were selected using the puromycin resistance gene that had been incorporated in the vector; and the surviving cells were further propagated in the presence of puromycin until confluent. The fibroblasts were then differentiated and matured to adipocytes according to the normal procedure. These 3T3-L1 adipocytes have reduced Fh protein levels but not complete knockout like the

immortalized MEF cells. Our laboratory has demonstrated that the accumulation of fumarate following *Fh* k/d results in increased succination of proteins when matured in normal (5 mM) glucose conditions (unpublished data). Subsequently succination increases independent of high glucose derived metabolic changes. The current experiment will likewise utilize *Fh* k/d adipocytes matured in 5 mM glucose to investigate succination and autophagy.

To evaluate compartment specific alterations in succination and autophagy, I will administer 25μM CQ 24 hours before harvesting cells. I will investigate the accumulation of succinated proteins in the total homogenate and enriched fractions of cytosolic, mitochondrial, and nuclear proteins. Following this I will evaluate the rate of autophagic flux both in total homogenate and mitochondrial fractions. I hypothesize succinated proteins will accumulate in the mitochondria of *Fh* k/d adipocytes compared to scrambled controls. As described previously, autophagic flux represents the amount of lysosomal degradation of proteins within the cell lysates and is measured by the accumulation of LC3-II in the presence of CQ. We previously observed that cells matured in high glucose have reduced autophagic flux compared to those matured in normal glucose (Chapter 2). Therefore, I propose that flux through autophagy will be altered in *Fh* k/d cells compared to their respective scrambled controls.

3.2. Results

Cells with *Fh* k/d have markedly more succination than those treated with a scrambled control virus (Figure 3.2, 2SC panel, lanes 1-6 versus 7-12). These total cell homogenates had no apparent change in protein succination upon

addition of CQ, though there was a slight increase in succination band density. Total cell lysates were then evaluated for Fh levels to demonstrate that the knockdown was efficient (Figure 3.2, Fumarase panel, lanes 1-6 versus 7-12). Next, the flux through autophagy was assessed by comparing adipocytes with and without CQ administration. The accumulation of LC3-II as a result of autophagic inhibition by CQ is a reliable measure of autophagic flux. These data demonstrate a trend for a decrease in autophagic flux in *Fh* k/d cells compared to scrambled controls (Figure 3.2, LC3 panel, lanes 4-6 minus 1-3 versus lanes 10-12 minus 7-9 and graph of densitometric analysis). We previously showed that autophagic flux is reduced in adipocytes matured in high glucose compared to normal glucose (Figure 2.2). It appears that *Fh*-deficient adipocytes also have reduced autophagic flux compared to scrambled controls.

The cellular protein profile was then assessed for compartment specific differences in protein succination and autophagic flux by generating fractions enriched in cellular organelles. Fractionation was assessed using markers for mitochondria, cytosol, and nucleus to demonstrate enrichment of those compartments (Figure 3.3, voltage dependent anion channel 2 [Vdac2], α-tubulin, and histone H3 panels respectively). High levels of succination are evident in the cytosolic, mitochondrial, and nuclear compartments (Figure 3.3, 2SC panel, lanes 1-6 compared to 7-12 compared to 13-18), but only the mitochondrial compartment demonstrates increased succinated protein levels following treatment with CQ (Figure 3.3, 2SC panel, lanes 7-9 versus 10-12). This increased accumulation of succinated proteins when autophagy was inhibited

indicates these proteins were turnover by autophagy in the mitochondria at a faster rate than the two other fractions. These data suggest that mitochondria accumulate and turn over proteins at a faster rate. These observations align with previous data in *Fh* deficient MEF cultures (unpublished data, Figure 3.1). We additionally evaluated the levels of Atg7 and observed that it was present predominantly in the cytosolic fraction (Figure 3.3, Atg7 panel lines 1-6), possibly because Atg7 accumulates with CQ administration in this cytosolic fraction (Figure 3.3, Atg7 panel, lines 4-6 versus 1-3).

To increase our understanding of the unique accumulation occurring in the mitochondrial enriched fraction, we further evaluated the *Fh* k/d lysates and compared them to scrambled control mitochondrial enriched fractions. We confirmed that *Fh* k/d lysates have markedly elevated succination compared to scrambled control (Figure 3.4, 2SC panel, lanes 7-12 versus 1-6). Additionally, the results clearly confirmed that mitochondrial enriched fractions accumulate more succinated proteins in the presence of CQ, demonstrating that these fractions contain more succinated proteins that are normally turned over more rapidly by autophagy (Figure 3.4, 2SC panel, lanes 10-12 versus 7-9). Despite this, assessment of flux through autophagy by evaluating mitochondrial LC3-II levels as above indicates that that there is a trend for a decreased rate of overall flux in *Fh* k/d cells compared to scrambled controls (Figure 3.5).

Succinated protein accumulation occurs in the *Fh* k/d model due to the accumulation of fumarate. I speculated that cells with reduced fumarase levels might accumulate other protein modifications such as succinylation which occurs

when succinyl-CoA, a derivative of a Krebs cycle intermediate, reacts with protein lysine residues. Increased back pressure on the Krebs cycle may permit succinyl-CoA accumulation and hence elevate levels of succinylation. We have previously demonstrated that there are no significant increases in succinylation in high glucose conditions compared to normal glucose (Manuel and Frizzell, 2013). The *Fh* k/d model likewise demonstrates succinylated-lysine is unchanged in scrambled control versus *Fh* k/d adipocytes and unchanged by the inhibition of autophagy with CQ (Figure 3.6, Succinyl-K panel). This indicates succinylated proteins do not accumulate in this model of reduced Krebs cycle flux and suggests they are not turned over by autophagy in the way that succinated proteins are.

3.3. Discussion

Fumarate accumulation due to a reduction in the tricarboxylic acid cycle enzyme fumarase leads to an increase in protein succination. We hypothesized that flux through autophagy might be altered as a result of *Fh* k/d. Our investigation demonstrated that there is a trend for a decrease in autophagic flux in the total homogenate of *Fh* k/d cells compared to scrambled controls (Figure 3.2). This trend is consistent with the reduced autophagic flux in high glucose conditions compared to normal glucose (Figure 2.2), suggesting that increased succination plays a role in decreasing normal levels of autophagic flux. Both these studies investigated 3T3-L1 adipocytes, but the *Fh* k/d cells may have alternative mechanisms of maintaining autophagic flux. As discussed in Chapter 2, Cathepsin B has been shown by mass spectrometry to be succinated in high

glucose conditions but not in normal glucose (unpublished data). This succination results in a decrease in Cathepsin B activity in high glucose treated adipocytes. While we speculated that *Fh* k/d adipocytes would also have reduced Cathepsin B activity, a preliminary investigation suggests that Cathepsin B activity is not reduced in *Fh* k/d cells despite their elevation in succinated protein levels compared to scrambled controls (unpublished data). A potential explanation for these enzymatic differences is that *Fh* k/d adipocytes increase Cathepsin B protein levels to compensate for reduced activity as a result of succination. Alternatively, the *Fh* k/d adipocytes may depend more on the activity of other cathepsin enzymes (e.g. Cathepsin D) even if Cathepsin B were also succinated in this model, perhaps on a cysteine reside that is non-essential for activity. Since the *Fh* k/d adipocytes have elevated succination compared to high glucose adipocytes, *Fh* k/d may also induce more pronounced metabolic adaptations due to elevated cellular stress as a result of succination.

Since mitochondria are the location of fumarate production, we predicted that succinated proteins would accumulate in the mitochondria of adipocytes. We previously demonstrated that succinated protein content was low in the mitochondria but accumulated in the presence of CQ in MEFs with *Fh* knock out (Figure 3.1). This indicates that succinated proteins in the mitochondrial rich fraction were turned over by autophagy. We then generated a 3T3-L1 adipocyte model of elevated succination by reducing *Fh* levels to investigate cellular fractions in a non-cancerous cell line. As anticipated, succinated proteins accumulate in the cytosolic and nuclear enriched fractions independent of CQ

administration (Figure 3.4, 2SC panel, lanes 1-6 and lanes 15-20). Additionally, *Fh* k/d adipocytes accumulate succinated proteins in the mitochondrial enriched fraction only in the presence of CQ as did the MEF cells (Figures 3.1 and 3.4). This heightened accumulation might be expected since mitochondria are the site of fumarate production. The rapid turnover in the mitochondria may mitigate mitochondrial damage and compensate for localized fumarate concentrations being high. Future experiments should delineate the role of the mitochondria further by investigating specific autophagy of the mitochondria, i.e. mitophagy (Lemasters, 2005, Kissova et al. 2004). Additionally, flux through autophagy is reduced in *Fh* k/d mitochondrial preparations compared to scrambled controls (Figure 3.5). Impairment of proper protein recycling through the lysosome leads to an accumulation of damaged cellular debris and may contribute to inflammation as described previously (Chapter 2). Our current results highlight that succinated proteins are turned over by autophagy in the mitochondrial enriched fraction of *Fh* k/d adipocytes, but it will be important to ensure that future fraction preparations are more organelle specific, separating mitochondria from any lysosomes or endoplasmic reticulum that may contaminate this fraction.

Levels of succinylation were not different in scrambled control and *Fh* k/d adipocytes (Figure 3.6, Succinyl-K panel, lanes 1-5 verses lanes 6-10). Succinyl-K was also unaltered when adipocytes were treated with the autophagy inhibitor CQ (Figure 2.6, Succinyl-K, lanes 1-2 verses 3-5 and lanes 6-8 verses 9-10). The lack succinylated protein accumulation in adipocytes is not surprising since succinyl-CoA levels are normally low in the mitochondria. Most work

documenting an increase has been observed in sirtuin (SIRT) 5 knockout models since SIRT 5 has been described as a desuccinylase (Park et al. 2013, Zhang et al. 2015). Succinyl-CoA levels may not accumulate even if the Krebs cycle was inhibited as long as the cells have a demand to produce GTP, favoring the hydrolysis of this this thioester. If succinylation accumulated it would have been interesting to determine if these modified proteins were turned over by autophagy similar to succinated proteins (in addition to the known turnover by SIRT 5). The lack of net change in succinylation in either cell type in the presence of CQ confirms that *Fh* k/d adipocytes uniquely increase succination without accumulating other acyl CoA derived protein modifications.

We conclude that reducing the levels of *Fh* in adipocytes using shRNA will increase succination and reduce flux through autophagy. As in the cell culture diabetic model, adipocytes with *Fh* k/d have an accumulation of LC3-II in the presence of CQ indicating a reduction in autophagic flux. The turnover of succinated proteins by autophagy is most pronounced in mitochondrial enriched fractions likely because the mitochondria are the site of the tricarboxylic acid cycle where fumarate is produced. This model may have utility for more specific investigations of succinated protein turnover in the mitochondria to examine mitophagy, i.e. autophagy of the mitochondria.

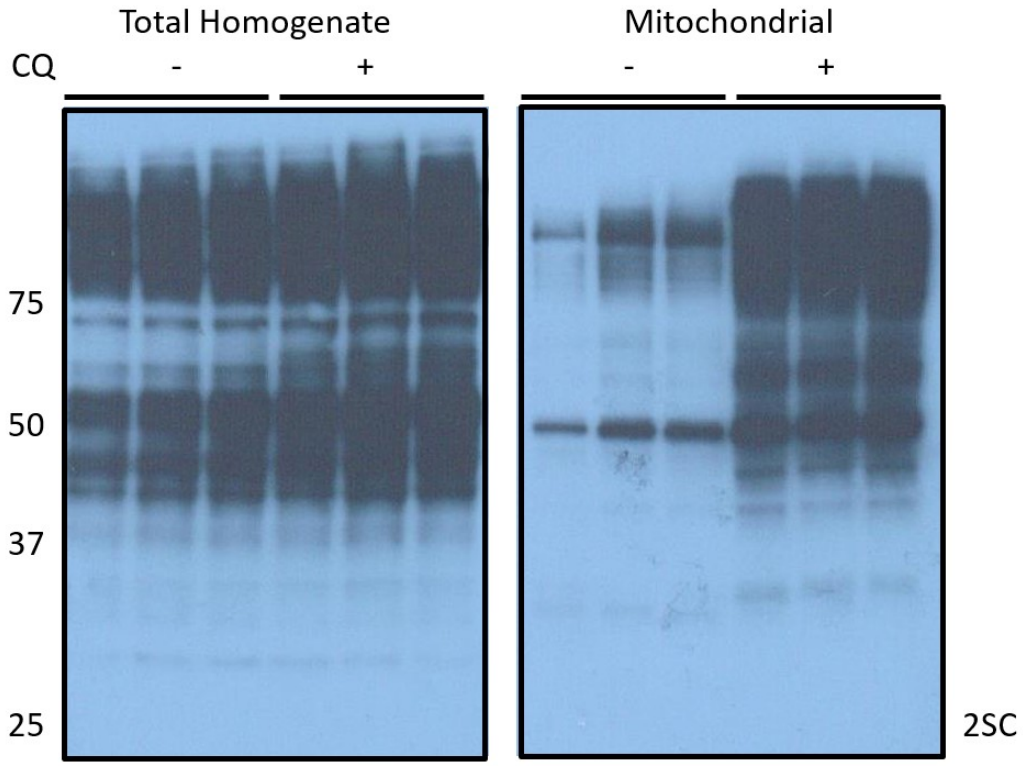

Figure 3.1. Succinated Protein Turnover in MEF Mitochondria. Murine embryonic fibroblasts (MEFs) from fumarase knockout mice treated with 25 μM chloroquine (CQ) for 18 hours to inhibit autophagy. Lysates were fractionated then assessed for protein succination. Total cell lysates have consistent levels of protein succination with and without CQ administration (**2SC left panel**). Mitochondrial enriched fractions have markedly increased succination in the presence of CQ (**2SC right panel**). Cellular fractions were separated by 1-D SDS PAGE (n=3 per group, 30 μg protein per lane). Molecular weight markers (kDa) are indicated on left.

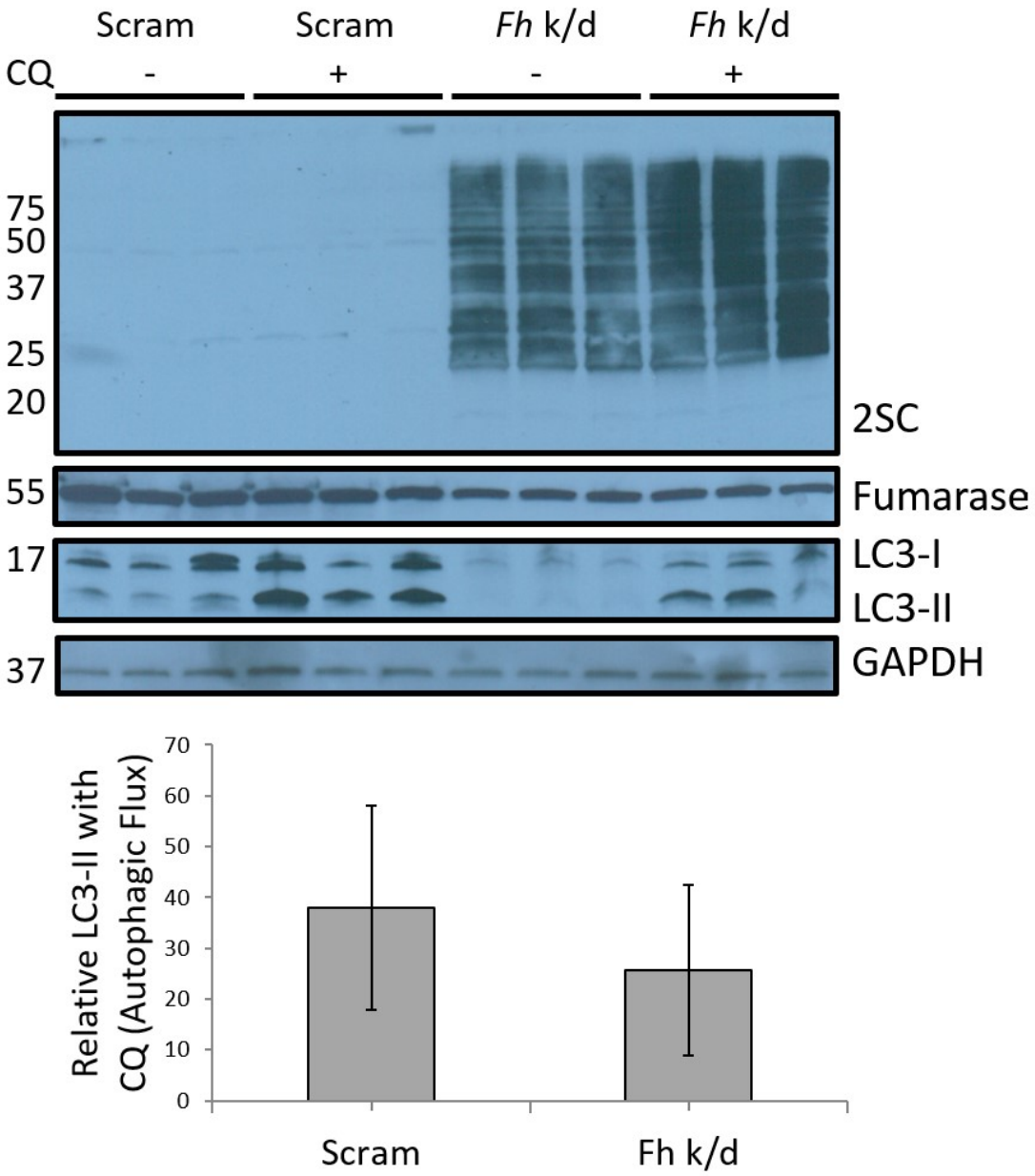

Figure 3.2. *Fh* k/d Protein Succination and Autophagic Flux. Adipocytes were transduced with scrambled control (scram) or fumarase knockdown (*Fh* k/d) shRNA and matured in 5 mM glucose conditions following selection with puromycin. Succination of proteins is markedly increased in *Fh* k/d cells compared to scram cells (**2SC panel**). Fumarase levels are reduced in the *Fh* k/d cells compared to the scram cells, confirming an effective reduction in fumarase levels (**Fumarase panel**). LC3-II accumulates in the presence of 25 μM CQ in both scram and *Fh* k/d samples (**LC3 panel**). GAPDH levels are indicated as a loading control (**GAPDH panel**). Flux through autophagy is quantified as the increase in LC3-II levels after CQ administration as determined by the densitometry (**Graph**). Total cell lysates, 30 μg protein per lane, were separated

by 1-D SDS PAGE (n=3 per group). Molecular weight markers (kDa) are indicated on left.

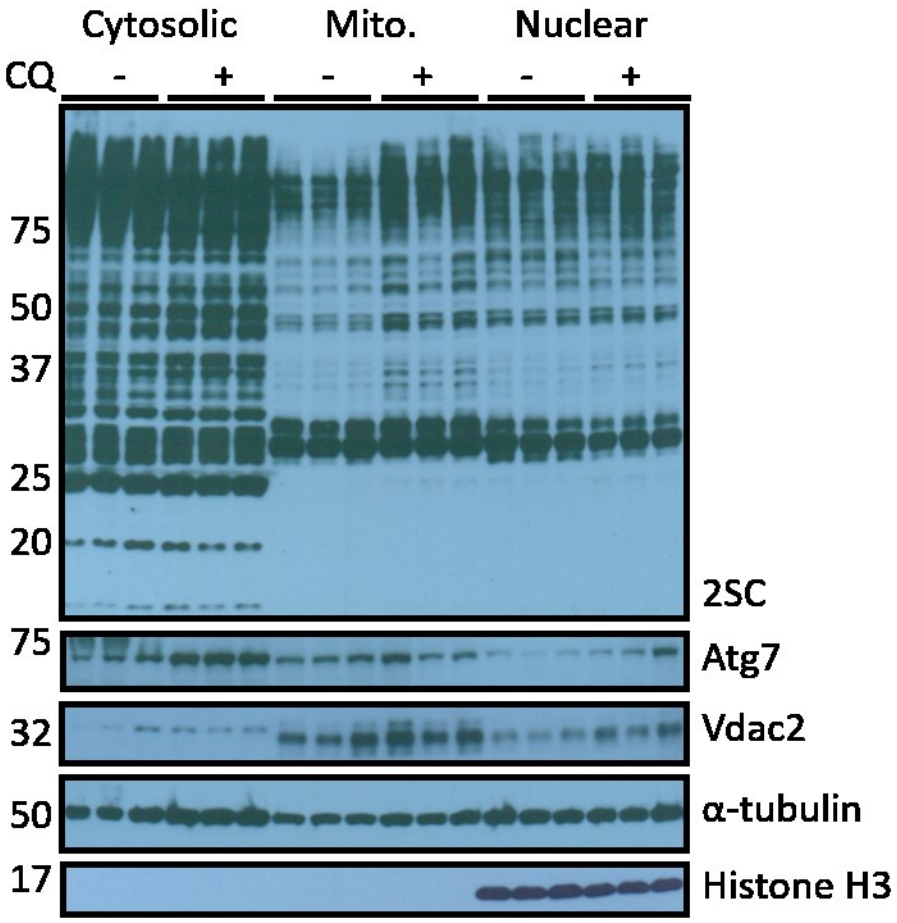

Figure 3.3. *Fh* k/d Protein Succination in Enriched Fractions. Cytosolic, Mitochondrial (Mito.), and Nuclear enriched fractions of fumarase knockdown (*Fh* k/d) adipocytes grown in 5 mM glucose with and without 25 μM CQ for 24 hours. Elevated levels of protein succination are present in all *Fh* k/d fractions. 2SC is increased markedly in the mitochondrial enriched fraction with CQ administration (**2SC panel**). Atg7 levels in the cytosolic fraction are increased in the presence of CQ (**Atg7 panel**). Vdac2 is indicated to demonstrate enrichment of mitochondrial fractions (**Vdac2 panel**). Tubulin is shown indicate total loading between groups (**α-tubulin panel**). Histone H3 is indicated to demonstrate enrichment of nuclear fractions (**Histone H3 panel**). Total cell lysates, 30 μg protein per lane, were separated by 1-D SDS PAGE (n=3 per group). Molecular weight markers (kDa) are indicated on left.

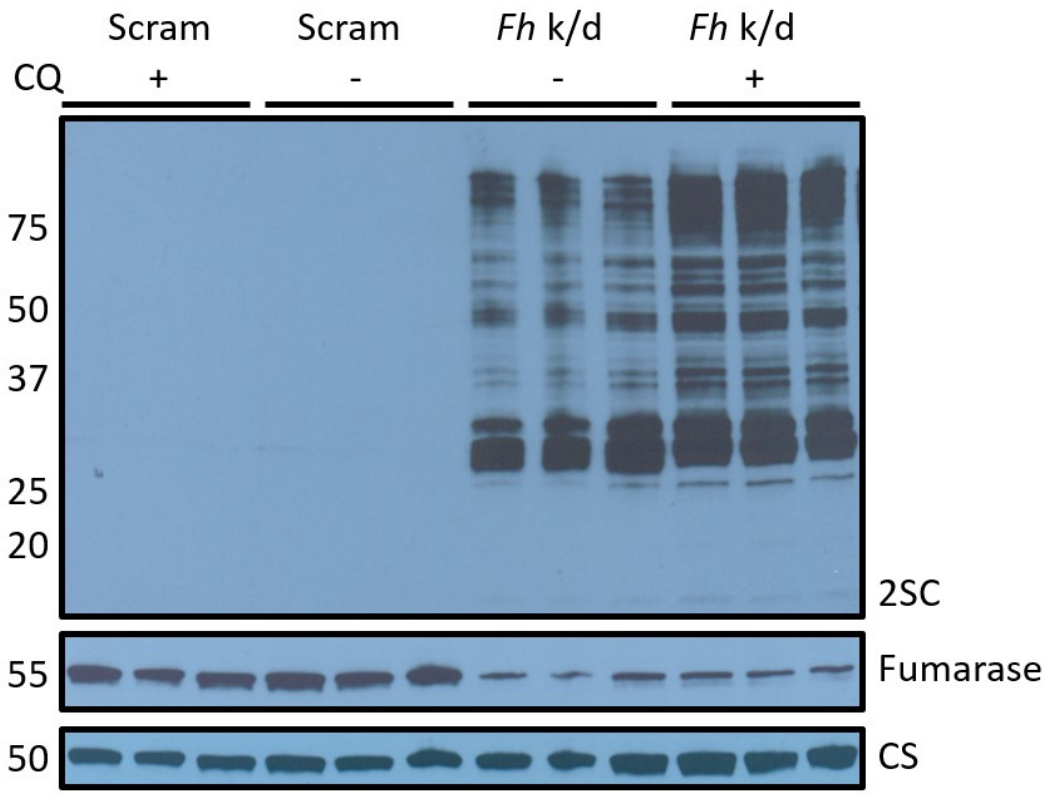

Figure 3.4. *Fh* k/d Protein Succination in Mitochondria. Mitochondrial enriched fractions of scrambled control (scram) and fumarase knockdown (*Fh* k/d) adipocyte samples with and without 25 μM CQ administration. Succination of proteins is present in the *Fh* k/d cells and increased in the presence of CQ (**2SC panel**). Reduced fumarase levels in the *Fh* k/d samples confirming the effectiveness of the shRNA knockdown (**Fumarase panel**). Citrate Synthase is shown as a mitochondrial loading control (**CS panel**). Total cell lysates, 30 μg protein per lane, were separated by 1-D SDS PAGE (n=3 per group). Molecular weight markers (kDa) are indicated on left.

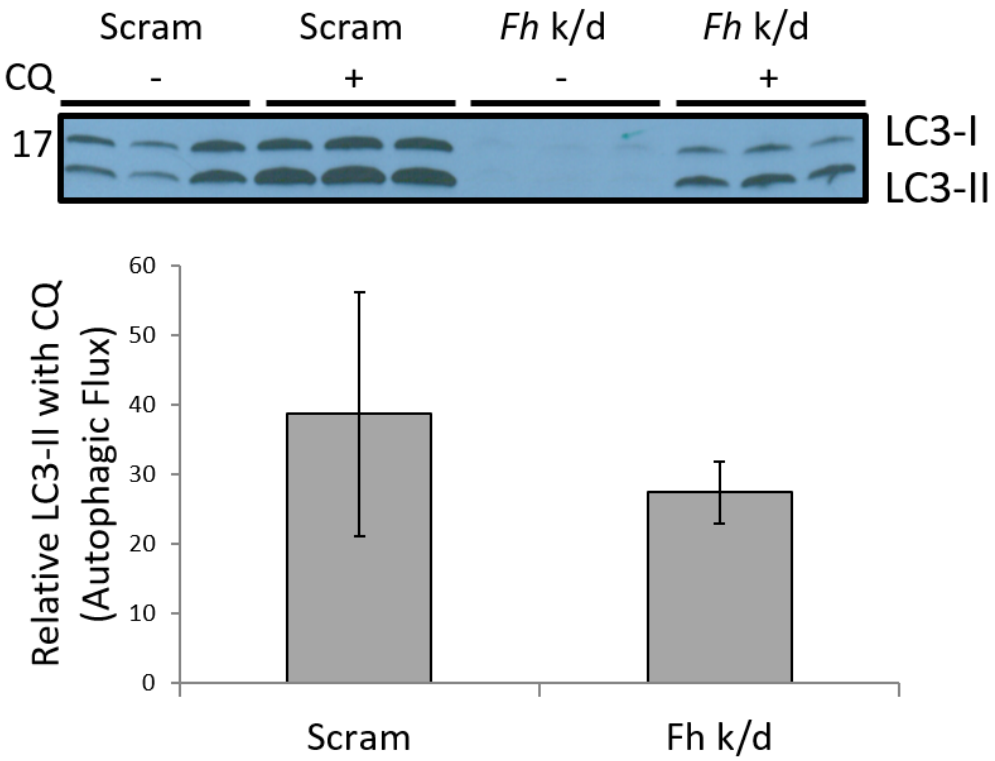

Figure 3.5. *Fh* k/d Autophagic Flux in Mitochondria. Mitochondrial enriched fractions of scrambled control (scram) and fumarase knockdown (*Fh* k/d) adipocyte samples with and without 25 μM CQ for 24 hours. LC3-II accumulation after CQ administration is a measure of autophagic flux (**LC3 panel**). Quantification of autophagic flux indicates a trend for a decreased flux in adipocytes that have *Fh* k/d (**Graph**). Total cell lysates, 10 μg protein per lane, were separated by 1-D SDS PAGE (n=3 per group). Molecular weight markers (kDa) are indicated on left.

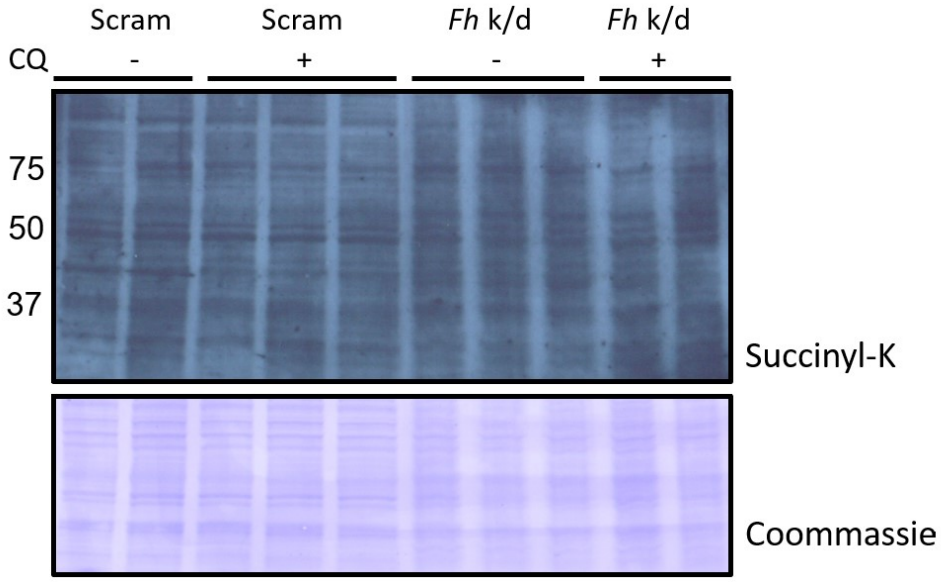

Figure 3.6. Succinylation in *Fh* k/d and Scrambled Control Adipocytes. Evaluation of protein modification by succinyl-CoA in fumarase knockdown (*Fh* k/d) adipocyte samples with and without 25 μM CQ administration. Succinylated lysine was assessed in total homogenate of scrambled control and *Fh* k/d samples. Protein modification by succinyl-CoA is not altered by CQ administration (**Succinyl-K panel**, n=2 or 3 per group). Total cell lysates, 30 μg protein per lane, were separated by 1-D SDS PAGE.

Chapter IV

FUTURE DIRECTIONS

These results highlight the importance of understanding adipocyte metabolism in context with protein succination and autophagy. The reduction in autophagic flux, as measured by LC3-II accumulation, resulting from high glucose induced cellular stress is a representation of metabolic dysregulation in diabetic conditions. Further investigation of autophagy in the context of diabetes should assess adipocytes extracted from the adipose tissue of *db/db* (diabetic) mice or similar models. Linking diabetes-induced elevations in 2SC to reductions in autophagic flux would further support the utility of protein succination as a marker of metabolic stress under a high glucose insult.

Continued investigation of the crucial autophagic protein Atg7 and the cathepsin proteins will help divulge the precise mechanism of autophagy inhibition under high glucose conditions. Delineating the succination state of Atg7 in high glucose conditions and assessing if its succination contributes to reduced autophagic flux. Since we know Cathepsin B is specifically succinated in high glucose when autophagic flux is reduced and that its activity levels are unaltered in *Fh* k/d adipocytes, further work should evaluate if Cathepsin B is succinated in the *Fh* k/d model. Additionally, measuring total protein levels of the major cathepsin proteins could assess for compensatory functions when Cathepsin B activity is reduced.

The 3T3-L1 adipocyte model of diabetes will continue to uncover metabolic pathways contributing to high glucose induced metabolic stress. An evaluation of succination and autophagic flux in cellular fractions of high glucose adipocytes can be used to understand the importance of the mitochondria in succinated protein turnover. In particular, preparation of cellular fractions that specifically separate the mitochondria from lysosomes and other organelles would ensure that 2SC accumulation in the mitochondrial enriched fraction is not due to accumulation within the lysosome in the presence of CQ. These investigations could ultimately be expanded to adipose tissue from diabetic patients to elucidate the connection between autophagic flux and accumulation of 2SC. As research on diabetes and protein succination progresses, it is increasingly evident that 2SC is a valuable marker of adipocyte metabolic stress.

Chapter V

MATERIALS AND METHODS

5.1. Cell Culture

3T3-L1 murine fibroblasts were purchased from American Type Culture Collection (Manassas, VA) and maintained up to 8 passages in DMEM containing 5 mM glucose, 10% Bovine Calf Serum (Thermo Scientific), 1% penicillin/streptomycin (CellGro) at 37^{o}C with 5% CO_2 and 95% humidity. Medium was changed every 2 days. At 70-80% confluence cells were trypsinized (Thermo Scientific), neutralized with excess medium and collected by centrifugation at 1,000 g for 5 min at 25^{o}C. The cells were then re-suspended in medium for a new passage.

3T3-L1 fibroblasts were seeded at densities of 50,000 and 100,000 cells/well for 6-well plates and 10 cm^2 petri dishes respectively. 3T3-L1 fibroblasts were induced to differentiate 24 hours post-confluence (~3-4 days) in DMEM with 10% Fetal Bovine Serum (Atlanta Biologicals), 1% penicillin/streptomycin, insulin (10 µg/mL), dexamethasone (0.3 µM), 3-isobutyl-1-methylxanthine (0.5 mM) and 30 mM glucose for 3 days. At day 0, differentiation medium was removed, cells were washed with PBS and maturation medium containing 5 mM/0.3 nM or 30 mM/3 nM glucose/insulin was applied. The medium was changed every 2 days and the adipocytes were matured in 5 mM or 30 mM glucose for 8 days. When the lysosomal inhibitor was

used, cells were treated with 25 μM chloroquine (Sigma Aldrich) at day 7 for 24 hours before collection. Cells cultured in 5 mM glucose were supplemented with 5 mM glucose daily and several hours prior to protein harvest to maintain glucose levels.

5.2. Protein Extraction from Adipocytes

All cellular protein was collected at day 8 by lysing the cells in radioimmunoprecipitation assay buffer (RIPA, Appendix A) and sonicated 3 times for 12-15 seconds each. Ice cold acetone, 9 x volume, was then added to the samples, vortexed, then allowed to sit on ice for 10 min. The samples were then vortexed again and centrifuged at 2,800 g for 10 min at 4^{o}C. The acetone was decanted and the samples re-suspended in 0.5-1 mL of RIPA buffer and sonicated 3 times for 10 seconds each. The protein concentration was determined using the Lowry assay (Appendix B).

5.3. Lentiviral Vector Production

The lentiviral vectors were prepared by the University of South Carolina Viral Vector Facility. Briefly, TRC2 Fh1 shRNA, clone- TRCN0000246831 or SHC202 MISSION TRC2 pLKO.5-puro non-mammalian shRNA control plasmids (Sigma/Aldrich, St. Louis, MO) were used to generate the lentiviral vectors. The vectors also contained a puromycin resistance gene. 15 μg vector plasmid, 10 μg psPAX2 packaging plasmid (Addgene 12260, Cambridge, MA), 5 μg pMD2.G envelope plasmid (Addgene 12259, Cambridge, MA) and 2.5 μg pRSV-Rev plasmid (Addgene 12253, Cambridge, MA) were transfected into 293T cells. The filtered conditioned medium was collected and stored at -80°C until use.

Lentiviral vectors were generated using a transient transfection protocol, as described previously (Kantor, 2011). Briefly, 15 µg vector plasmid, 10 µg psPAX2 packaging plasmid (Addgene #12260), 5 µg pMD2.G envelope plasmid (Addgene #12259) and 2.5 µg pRSV-Rev plasmid (Addgene #12253) were introduced into 293T cells by transfection. Vector particles were collected in filtered conditioned medium at 72 hour post-transfection. Vector and viral stocks were aliquoted and stored at -80 °C.

5.4. Lentiviral Transduction

3T3-L1 fibroblasts were grown in 1 g/L glucose DMEM with 10% FCS and 1% penicillin streptomycin until 90% confluent on 10 cm^2 petri dishes. The fibroblasts were incubated overnight with 5 mL of filtered conditioned medium containing 150 µL Fh-1 shRNA or control virus. Successfully transduced fibroblasts were selected using 2.5 µg/mL puromycin, supplemented in the medium every 48 hours. The selected fibroblasts were propagated until confluent, then differentiated to adipocytes and matured for 8 days in 5 mM glucose as described above. In some cases the adipocytes were treated with 25 µM chloroquine for 24 hours before the cells were harvested into fractions as described below.

5.5. Cellular Fractionation

Mitochondrial enriched preparations were collected by harvesting cells in homogenization buffer (Appendix A). The cells were washed 3 times in ice-cold PBS prior to scraping in homogenization buffer. Each sample was homogenized on ice with a glass homogenizer 20 times, then passed through a 25 gauge

needle 5 times. 150 µL of total homogenate was collected in a separate tube, and then the remaining sample volume was centrifuged at 500 g for 10 min to generate the nuclear pellet. The supernatant was placed in a clean tube and centrifuged at 18,000 g for 20 min to generate the mitochondrial pellet. The resulting supernatant was then collected as the cytosolic fraction. Nuclear and mitochondrial pellets were re-suspended in RIPA buffer; then all fractions were processed and quantified as described above.

5.6. Western Immunoblotting

Samples were prepared using 10-30 µg protein with the addition of 4x Laemmli reducing buffer, boiled at 95^{o}C, pulse centrifuged, loaded on 7.5%, 12%, or 18% Tris-Glycine gel (TGX, Biorad), and electrophoresed at 200 V for 60 min at room temperature. The protein was transferred to a PVDF membrane in transfer buffer at 250 mA for 100 min at 4 ^{o}C. The membrane was stained with Ponceau Red, and then blocked in 5% non-fat milk or 5% bovine serum albumin (BSA) according to the antibody manufacturer's recommendations. Membranes were probed using primary polyclonal anti-2SC antibody, prepared as described previously (Nagai et al. 2007). The anti-Atg7 (#8558), anti-citrate-synthase (#14309), anti-fumarase (#4567), anti-LC3 (#2775), and anti-α-tubulin [DM1A] (#3873) primary antibodies used were from Cell Signaling (Cell Signaling, Beverly, MA). The anti-GAPDH (#FL-335) primary antibody was from Santa Cruz (Santa Cruz Biotechnology, Dallas, TX). The anti-Histone H3 (#05-928) primary antibody was from EMD Millipore (EMD Millipore, Darmstadt, Germany). The anti-VDAC2 (#GTX104745) primary antibody was from GeneTex (GeneTex,

Irvine, CA). Horse radish peroxidase (HRP) labeled secondary antibodies were used to detect the protein (Cell Signaling). Pierce® ECL 2 Western Blotting Substrate was used to detect a chemiluminescent signal on photographic film (Denville Scientific, Metuchen, NJ). ImageJ software (NIH) was used to quantify band intensity by densitometry and normalize to α-tubulin levels.

5.7. Immunoprecipitation

Atg7 was immunoprecipitated from 400 µg of 5 mM and 30 mM glucose treated cell lysates using a polyclonal anti-Atg 7 antibody (Cell Signaling #8558). Samples were diluted in 400 µL RIPA buffer with 2 µL protease inhibitors and pre-cleared with 10 µL Protein G magnetic beads (BioRad) on a Roto-Torque (Cole-Parmer, Vernon Hills, IL) for 30 min at room temperature. 10 µL Protein G magnetic beads were simultaneously incubated with 1.09 µg anti-Atg7 antibody for 30 min at room temperature on the Roto-Torque. Following centrifugation of the pre-cleared sample at 4000 x g for 2 min in a Heraeus Biofuge 13 microcentrifuge (Thermo Fisher Scientific), the samples were placed in magnetic holder for 3 min. The supernatant was removed and added to the bead-antibody complex and placed on the Roto-Torque for 35 min at room temperature. The resulting bead-antibody-antigen complex was washed 3 times in 50 mM phosphate buffer, pH 7.4, then re-suspended in 30 µL water with 8 µL Laemmli loading buffer. The samples were boiled to separate the magnetic beads from the protein-antibody complex and the supernatant was analyzed using one-dimensional SDS-PAGE as described above. The immunoblots were probed with polyclonal anti-2SC and anti-Atg7 antibodies.

5.8. Data Analysis

Densitometric quantifications were performed in ImageJ (NIH). All graphs were generated in Microsoft Excel.

References

1. Alderson NL, Wang Y, Blatnik M, Frizzell N, Walla MD, Lyons TJ, Alt N, Carson JA, Nagai R, Thorpe SR, Baynes JW. S-(2-succinyl)cysteine: A novel chemical modification of tissue proteins by a krebs cycle intermediate. Arch Biochem Biophys. 2006 Jun 1;450(1):1-8.

2. Alkhouri N, Gornicka A, Berk MP, Thapaliya S, Dixon LJ, Kashyap S, Schauer PR, Feldstein AE. Adipocyte apoptosis, a link between obesity, insulin resistance, and hepatic steatosis. J Biol Chem. 2010 Jan 29;285(5):3428-38.

3. Ashrafian H, O'Flaherty L, Adam J, Steeples V, Chung YL, East P, Vanharanta S, Lehtonen H, Nye E, Hatipoglu E, Miranda M, Howarth K, Shukla D, Troy H, Griffiths J, Spencer-Dene B, Yusuf M, Volpi E, Maxwell PH, Stamp G, Poulsom R, Pugh CW, Costa B, Bardella C, Di Renzo MF, Kotlikoff MI, Launonen V, Aaltonen L, El-Bahrawy M, Tomlinson I, Pollard PJ. Expression profiling in progressive stages of fumarate-hydratase deficiency: The contribution of metabolic changes to tumorigenesis. Cancer Res. 2010 Nov 15;70(22):9153-65.

4. Bardella C, El-Bahrawy M, Frizzell N, Adam J, Ternette N, Hatipoglu E, Howarth K, O'Flaherty L, Roberts I, Turner G, Taylor J, Giaslakiotis K, Macaulay VM, Harris AL, Chandra A, Lehtonen HJ, Launonen V, Aaltonen LA, Pugh CW, Mihai R, Trudgian D, Kessler B, Baynes JW, Ratcliffe PJ,

Tomlinson IP, Pollard PJ. Aberrant succination of proteins in fumarate hydratase-deficient mice and HLRCC patients is a robust biomarker of mutation status. J Pathol. 2011 Sep;225(1):4-11.

5. Blatnik M, Thorpe SR, Baynes JW. Succination of proteins by fumarate: Mechanism of inactivation of glyceraldehyde-3-phosphate dehydrogenase in diabetes. Ann N Y Acad Sci. 2008 Apr;1126:272-5.

6. Cancello R, Henegar C, Viguerie N, Taleb S, Poitou C, Rouault C, Coupaye M, Pelloux V, Hugol D, Bouillot JL, Bouloumie A, Barbatelli G, Cinti S, Svensson PA, Barsh GS, Zucker JD, Basdevant A, Langin D, Clement K. Reduction of macrophage infiltration and chemoattractant gene expression changes in white adipose tissue of morbidly obese subjects after surgery-induced weight loss. Diabetes. 2005 Aug;54(8):2277-86.

7. Castro-Vega LJ, Buffet A, De Cubas AA, Cascon A, Menara M, Khalifa E, Amar L, Azriel S, Bourdeau I, Chabre O, Curras-Freixes M, Franco-Vidal V, Guillaud-Bataille M, Simian C, Morin A, Leton R, Gomez-Grana A, Pollard PJ, Rustin P, Robledo M, Favier J, Gimenez-Roqueplo AP. Germline mutations in FH confer predisposition to malignant pheochromocytomas and paragangliomas. Hum Mol Genet. 2014 May 1;23(9):2440-6.

8. Center for Disease Control and Prevention. National Diabetes Statistics Report: Estimates of Diabetes and Its Burden in the United States, 2014 [Internet]. Atlanta, GA

9. Ceperuelo-Mallafre V, Ejarque M, Serena C, Duran X, Montori-Grau M, Rodriguez MA, Yanes O, Nunez-Roa C, Roche K, Puthanveetil P, Garrido-Sanchez L, Saez E, Tinahones FJ, Garcia-Roves PM, Gomez-Foix AM, Saltiel AR, Vendrell J, Fernandez-Veledo S. Adipose tissue glycogen accumulation is associated with obesity-linked inflammation in humans. Mol Metab. 2015 Oct 16;5(1):5-18.

10. Choo HJ, Kim JH, Kwon OB, Lee CS, Mun JY, Han SS, Yoon YS, Yoon G, Choi KM, Ko YG. Mitochondria are impaired in the adipocytes of type 2 diabetic mice. Diabetologia. 2006 Apr;49(4):784-91.

11. Diez JJ, Iglesias P. The role of the novel adipocyte-derived hormone adiponectin in human disease. Eur J Endocrinol. 2003 Mar;148(3):293-300.

12. Frizzell N, Rajesh M, Jepson MJ, Nagai R, Carson JA, Thorpe SR, Baynes JW. Succination of thiol groups in adipose tissue proteins in diabetes: Succination inhibits polymerization and secretion of adiponectin. J Biol Chem. 2009 Sep 18;284(38):25772-81.

13. Frizzell N, Thomas SA, Carson JA, Baynes JW. Mitochondrial stress causes increased succination of proteins in adipocytes in response to glucotoxicity. Biochem J. 2012 Jul 15;445(2):247-54.

14. Geisler S, Holmstrom KM, Skujat D, Fiesel FC, Rothfuss OC, Kahle PJ, Springer W. PINK1/Parkin-mediated mitophagy is dependent on VDAC1 and p62/SQSTM1. Nat Cell Biol. 2010 Feb;12(2):119-31.

15. Giordano A, Murano I, Mondini E, Perugini J, Smorlesi A, Severi I, Barazzoni R, Scherer PE, Cinti S. Obese adipocytes show ultrastructural features of stressed cells and die of pyroptosis. J Lipid Res. 2013 Sep;54(9):2423-36.
16. Glick D, Barth S, Macleod KF. Autophagy: Cellular and molecular mechanisms. J Pathol. 2010 May;221(1):3-12.
17. Green H, Kehinde O. An established preadipose cell line and its differentiation in culture. II. factors affecting the adipose conversion. Cell. 1975 May;5(1):19-27.
18. Gregor MF, Hotamisligil GS. Thematic review series: Adipocyte biology. adipocyte stress: The endoplasmic reticulum and metabolic disease. J Lipid Res. 2007 Sep;48(9):1905-14.
19. Grimsrud PA, Picklo MJ S, Griffin TJ, Bernlohr DA. Carbonylation of adipose proteins in obesity and insulin resistance: Identification of adipocyte fatty acid-binding protein as a cellular target of 4-hydroxynonenal. Mol Cell Proteomics. 2007 Apr;6(4):624-37.
20. Halberg N, Khan T, Trujillo ME, Wernstedt-Asterholm I, Attie AD, Sherwani S, Wang ZV, Landskroner-Eiger S, Dineen S, Magalang UJ, Brekken RA, Scherer PE. Hypoxia-inducible factor 1alpha induces fibrosis and insulin resistance in white adipose tissue. Mol Cell Biol. 2009 Aug;29(16):4467-83.
21. Illy C, Quraishi O, Wang J, Purisima E, Vernet T, Mort JS. Role of the occluding loop in cathepsin B activity. J Biol Chem. 1997 Jan 10;272(2):1197-202.

22. Jin S. Autophagy, mitochondrial quality control, and oncogenesis. Autophagy. 2006 Apr-Jun;2(2):80-4.

23. Kantor B, Bayer M, Ma H, Samulski J, Li C, McCown T, Kafri T. Notable reduction in illegitimate integration mediated by a PPT-deleted, nonintegrating lentiviral vector. Mol Ther. 2011 Mar;19(3):547-56.

24. Keller MP, Attie AD. Physiological insights gained from gene expression analysis in obesity and diabetes. Annu Rev Nutr. 2010 Aug 21;30:341-64.

25. Kissova I, Deffieu M, Manon S, Camougrand N. Uth1p is involved in the autophagic degradation of mitochondria. J Biol Chem. 2004 Sep 10;279(37):39068-74.

26. Klionsky DJ, Eskelinen EL, Deretic V. Autophagosomes, phagosomes, autolysosomes, phagolysosomes, autophagolysosomes... wait, I'm confused. Autophagy. 2014 Apr;10(4):549-51.

27. Konige M, Wang H, Sztalryd C. Role of adipose specific lipid droplet proteins in maintaining whole body energy homeostasis. Biochim Biophys Acta. 2014 Mar;1842(3):393-401.

28. Lehmann JM, Moore LB, Smith-Oliver TA, Wilkison WO, Willson TM, Kliewer SA. An antidiabetic thiazolidinedione is a high affinity ligand for peroxisome proliferator-activated receptor gamma (PPAR gamma). J Biol Chem. 1995 Jun 2;270(22):12953-6.

29. Lemasters JJ. Selective mitochondrial autophagy, or mitophagy, as a targeted defense against oxidative stress, mitochondrial dysfunction, and aging. Rejuvenation Res. 2005 Spring;8(1):3-5.

30. Lin Y, Berg AH, Iyengar P, Lam TK, Giacca A, Combs TP, Rajala MW, Du X, Rollman B, Li W, Hawkins M, Barzilai N, Rhodes CJ, Fantus IG, Brownlee M, Scherer PE. The hyperglycemia-induced inflammatory response in adipocytes: The role of reactive oxygen species. J Biol Chem. 2005 Feb 11;280(6):4617-26.

31. Manuel AM, Frizzell N. Adipocyte protein modification by krebs cycle intermediates and fumarate ester-derived succination. Amino Acids. 2013 Nov;45(5):1243-7.

32. Mayerson AB, Hundal RS, Dufour S, Lebon V, Befroy D, Cline GW, Enocksson S, Inzucchi SE, Shulman GI, Petersen KF. The effects of rosiglitazone on insulin sensitivity, lipolysis, and hepatic and skeletal muscle triglyceride content in patients with type 2 diabetes. Diabetes. 2002 Mar;51(3):797-802.

33. Mazure NM, Pouyssegur J. Hypoxia-induced autophagy: Cell death or cell survival? Curr Opin Cell Biol. 2010 Apr;22(2):177-80.

34. Merkley ED, Metz TO, Smith RD, Baynes JW, Frizzell N. The succinated proteome. Mass Spectrom Rev. 2014 Mar-Apr;33(2):98-109.

35. Nagai R, Brock JW, Blatnik M, Baatz JE, Bethard J, Walla MD, Thorpe SR, Baynes JW, Frizzell N. Succination of protein thiols during adipocyte maturation: A biomarker of mitochondrial stress. J Biol Chem. 2007 Nov 23;282(47):34219-28.

36. Pajvani UB, Hawkins M, Combs TP, Rajala MW, Doebber T, Berger JP, Wagner JA, Wu M, Knopps A, Xiang AH, Utzschneider KM, Kahn SE,

Olefsky JM, Buchanan TA, Scherer PE. Complex distribution, not absolute amount of adiponectin, correlates with thiazolidinedione-mediated improvement in insulin sensitivity. J Biol Chem. 2004 Mar 26;279(13):12152-62.

37. Pareja-Galeano H, Santos-Lozano A, Sanchis-Gomar F, Fiuza-Luces C, Garatachea N, Galvez BG, Lucia A, Emanuele E. Circulating leptin and adiponectin concentrations in healthy exceptional longevity. Mech Ageing Dev. 2016 Mar 2

38. Petersen KF, Dufour S, Befroy D, Lehrke M, Hendler RE, Shulman GI. Reversal of nonalcoholic hepatic steatosis, hepatic insulin resistance, and hyperglycemia by moderate weight reduction in patients with type 2 diabetes. Diabetes. 2005 Mar;54(3):603-8.

39. Pollard PJ, Briere JJ, Alam NA, Barwell J, Barclay E, Wortham NC, Hunt T, Mitchell M, Olpin S, Moat SJ, Hargreaves IP, Heales SJ, Chung YL, Griffiths JR, Dalgleish A, McGrath JA, Gleeson MJ, Hodgson SV, Poulsom R, Rustin P, Tomlinson IP. Accumulation of krebs cycle intermediates and over-expression of HIF1alpha in tumours which result from germline FH and SDH mutations. Hum Mol Genet. 2005 Aug 1;14(15):2231-9.

40. Popelka H, Klionsky DJ. One step closer to understanding mammalian macroautophagy initiation: Interplay of 2 HORMA architectures in the ULK1 complex. Autophagy. 2015 Nov 2;11(11):1953-5.

41. Qiao S, Dennis M, Song X, Vadysirisack DD, Salunke D, Nash Z, Yang Z, Liesa M, Yoshioka J, Matsuzawa S, Shirihai OS, Lee RT, Reed JC, Ellisen

LW. A REDD1/TXNIP pro-oxidant complex regulates ATG4B activity to control stress-induced autophagy and sustain exercise capacity. Nat Commun. 2015 Apr 28;6:7014.

42. Singh PK, Singh S. Changing shapes of glycogen-autophagy nexus in neurons: Perspective from a rare epilepsy. Front Neurol. 2015 Feb 4;6:14.

43. Sinha R, Dufour S, Petersen KF, LeBon V, Enoksson S, Ma YZ, Savoye M, Rothman DL, Shulman GI, Caprio S. Assessment of skeletal muscle triglyceride content by (1)H nuclear magnetic resonance spectroscopy in lean and obese adolescents: Relationships to insulin sensitivity, total body fat, and central adiposity. Diabetes. 2002 Apr;51(4):1022-7.

44. Soussi H, Reggio S, Alili R, Prado C, Mutel S, Pini M, Rouault C, Clement K, Dugail I. DAPK2 downregulation associates with attenuated adipocyte autophagic clearance in human obesity. Diabetes. 2015 Oct;64(10):3452-63.

45. Sugii S, Olson P, Sears DD, Saberi M, Atkins AR, Barish GD, Hong SH, Castro GL, Yin YQ, Nelson MC, Hsiao G, Greaves DR, Downes M, Yu RT, Olefsky JM, Evans RM. PPARgamma activation in adipocytes is sufficient for systemic insulin sensitization. Proc Natl Acad Sci U S A. 2009 Dec 29;106(52):22504-9.

46. Sun K, Halberg N, Khan M, Magalang UJ, Scherer PE. Selective inhibition of hypoxia-inducible factor 1alpha ameliorates adipose tissue dysfunction. Mol Cell Biol. 2013 Mar;33(5):904-17.

47. Tang H, Sebastian BM, Axhemi A, Chen X, Hillian AD, Jacobsen DW, Nagy LE. Ethanol-induced oxidative stress via the CYP2E1 pathway disrupts adiponectin secretion from adipocytes. Alcohol Clin Exp Res. 2012 Feb;36(2):214-22.

48. Tanida I, Ueno T, Kominami E. LC3 and autophagy. Methods Mol Biol. 2008;445:77-88.

49. Ternette N, Yang M, Laroyia M, Kitagawa M, O'Flaherty L, Wolhulter K, Igarashi K, Saito K, Kato K, Fischer R, Berquand A, Kessler BM, Lappin T, Frizzell N, Soga T, Adam J, Pollard PJ. Inhibition of mitochondrial aconitase by succination in fumarate hydratase deficiency. Cell Rep. 2013 Mar 28;3(3):689-700.

50. Thomas SA, Storey KB, Baynes JW, Frizzell N. Tissue distribution of S-(2-succino)cysteine (2SC), a biomarker of mitochondrial stress in obesity and diabetes. Obesity (Silver Spring). 2012 Feb;20(2):263-9.

51. Weidberg H, Shpilka T, Shvets E, Abada A, Shimron F, Elazar Z. LC3 and GATE-16 N termini mediate membrane fusion processes required for autophagosome biogenesis. Dev Cell. 2011 Apr 19;20(4):444-54.

52. Zheng L, Cardaci S, Jerby L, MacKenzie ED, Sciacovelli M, Johnson TI, Gaude E, King A, Leach JD, Edrada-Ebel R, Hedley A, Morrice NA, Kalna G, Blyth K, Ruppin E, Frezza C, Gottlieb E. Fumarate induces redox-dependent senescence by modifying glutathione metabolism. Nat Commun. 2015 Jan 23;6:6001.

Appendix A

BUFFER PREPARATIONS

A.1. Homogenization Buffer

The buffer was prepared in 50 mL stocks containing 10 mM Tris Base, 10 mM MOPS, 1 mM EGTA, and 1 mM DTPA at pH 7.4 then 0.2 M sucrose was added. On day of use, 2 mM sodium orthovanadate, 2 mM sodium fluoride and protease inhibitor (1:1000) was added to the buffer. The buffer was stored at 4^{o}C.

A.2. RIPA Buffer

The buffer was prepared in 200 mL stocks containing 50 mM Tris-HCl pH 8, 150 mM NaCl, 1% Triton-X, 0.5% sodium deoxycholate, 0.1% SDS, and 2 mM EDTA. On day of use, 2 mM sodium orthovanadate, 2 mM sodium fluoride and protease inhibitor (1:1000) was added to the buffer. The buffer was stored at 4^{o}C.

A.3. Running Buffer

One liter of 10x stock was prepared containing 250 mM Tris-HCl, 1920 mM glycine and 10% (SDS). Working solution contains 100 mL of 10x stock diluted to 1 L with water.

A.4. Transfer Buffer

One liter of 10X stock was prepared containing 250 mM Tris-HCl, 1920 mM glycine. Working solution for transfer process contains 1x transfer buffer with 20% methanol.

A.5. Wash Buffer

One liter of 10x stock was prepared containing 200 mM Tris-HCl, pH 7.4. Tween-20 was added at 0.05% to 1x was buffer.

Appendix B

LOWRY ASSAY

Pipette the specific amounts of reagents into the microplate in the order listed. All samples are prepared in duplicates.

Table B.1: Preparation of BSA standard curve for the Lowry assay.

Probe	BSA (µL)	H20 (µL)	Copper Reagent (µL)	Incubation	Folin-Ciocolateu (µL)	Incubation
Blank	0	20	20	20 minutes at 37°C	60	30 minutes at 37°C
1	1	19	20		60	
2	2	18	20		60	
3	3	17	20		60	
4	4	16	20		60	
5	8	12	20		60	
6	10	10	20		60	
7	20	0	20		60	
Sample	5	15	20		60	

Stock BSA: Dissolve 50 mg BSA (Bovine Serum Albumin) in 10 mL deionized water to get 5 mg/mL stock/working solution.

Working Solutions: Dilute 400 µL of 5 mg/mL stock in 600 µL water to get 2 mg/mL solution.

Table B.2: Preparation of copper reagent for Lowry assay.

Stock Solution	Working Solution
Copper Sulfate 1% (w:v)	100 µL
Sodium Tartrate 2% (w:v)	100 µL
Sodium Carbonate 10% (w:v) in 0.5 M NaOH	2 mL

Folin-Ciocolateu Phenol Reagent: Purchased as a 2 N stock solution. For working solution at 500 µL of stock solution to 5.5 mL of water

Read absorbance at 660nm.

Appendix C

WESTERN BLOTTING

C.1. Gel Electrophoresis

1. After determining the protein content from the Lowry assay, 10-40 µg of protein was dissolved in water and 5 µL of Laemmli loading buffer was added.

2. Boil the samples for 15 min at 95°C then flash centrifuge.

3. Remove tape and comb from Bio-Rad pre cast Criterion gel and place in cassette.

4. Fill the cassette tank and gel with Tris/Glycine/SDS running buffer.

5. Load the samples into their individual lanes and 10 µL of marker into your lane of choice.

6. Run the gel at 200 V for 60 min.

C.2. Wet Transfer

1. Remove the gel from the pre-cast and cut to size

2. Soak the gel in Tris/Glycine/Methanol transfer buffer for 15 min.

3. Charge the PVDF membrane for ~1 minute in methanol. Soak the 2 pieces of

blotting paper, 2 sponges, and the membrane in Tris/Glycine/methanol for 15 min.

4. Assemble the transfer apparatus, starting with the black side first. Keep all materials soaking in transfer buffer during the assembly.

5. Place the sponge flat on the black side, followed by a piece of blotting paper. Next, place the gel on top followed by the PVDF membrane. Roll out any air bubbles between the gel and membrane using a roller. Finally, put the remaining piece of blotting paper on top of the membrane and the sponge on top.

6. Assemble the apparatus and transfer at 250 mA for 100 min or 40 mA for at least 12 hours.

7. Remove the membrane from the apparatus and wash with nanopure water.

8. Place the membrane in ponceau stain for 5 min then wash with nanopure water to visualize the bands. Inspect the membrane for equal loading and where bubbles formed during the transfer process. Wash the ponceau stain off the membrane with Tris-HCl wash buffer.

9. Block the membrane in 5% non-fat dry milk or 5% BSA for at least 1hr.

C.3. Immunostaining

1. Prepare 1% milk by diluting the 5% milk 1:4 in Tris-HCl wash buffer or prepare 5% BSA.

2. Add antibody to the milk or BSA in a 1:2000-1:10,000 dilution, see manufacturer instruction. Incubate for at least 1 hour on the rocker.

3. Pour off the antibody and wash the membrane 3 times in 1x wash buffer for 5 min each.

4. Add secondary antibody (anti-rabbit or anti-mouse) to 1% milk or 5% BSA in a 1:500-20,000 dilution and incubate for 1hr at room temperature.

5. Pour off the milk or BSA and was the membrane 3 times for 5 min each in wash buffer.

C.4. Developing Film

1. Prepare ECL solution by adding solution B to solution A and in a 1:40 dilution.

2. Add the ECL to the membrane and incubate for 5 min. Place the membrane in the cassette and cover with plastic wrap.

3. In the dark room, place a piece of X-ray film over the membrane then develop. Inspect the film after it has developed and adjust the exposure times accordingly.